Charles University

Faculty of Pharmacy in Hradec Králové

Department of Biological and Medical Sciences

Pharmacological modulation of endoglin expression in the liver in an animal model of nonalcoholic steatohepatitis

(Diploma thesis)

Supervisor: prof. PharmDr. Petr Nachtigal, Ph.D.

Hradec Králové 2024 Sepideh Moeini

Author’s Declaration

I, Sepideh Moeini, hereby declare that this master's diploma thesis entitled **" Pharmacological modulation of endoglin expression in the liver in an animal model of nonalcoholic steatohepatitis"** is my own original work, conducted under the guidance of prof. PharmDr. Petr Nachtigal, Ph.D., at Charles university faculty of pharmacy in Hradce Kralove. All sources of information and material I used during the research and writing of this thesis have been duly acknowledged and referenced.

Date: Signature:

Acknowledgment

First and foremost, I would like to express my deepest gratitude to my supervisor, Prof. PharmDr. Petr Nachtigal, Ph.D., for his invaluable guidance, unwavering support, and encouragement throughout the duration of this research. His expertise, insightful feedback, and constructive criticism have been instrumental in shaping this thesis.

I would also like to extend my appreciation to M.Sc. Samira Eissazadeh, my thesis consultant, for her time, expertise, and valuable feedback during the review process, as well as for providing experimental methods and laboratory guidelines.

I am thankful to the faculty and staff of the Faculty of Pharmacy at Charles University for providing a conducive learning environment and the necessary resources for the completion of this study.

Special thanks to my best friend, PharmDr. Navid Sharif, who has been a constant source of motivation, support, and encouragement throughout this journey. Your camaraderie and insightful discussions have enriched my research experience.

Lastly, I would like to express my heartfelt gratitude to my family for their unconditional love, support, and belief in my abilities. Their encouragement and sacrifices have been the driving force behind my academic pursuits.

Abstract

The liver plays a central role in human physiology, and its vulnerability to metabolic disorders such as non-alcoholic steatohepatitis (NADH) underscores the need for effective therapeutic interventions. This thesis investigates the potential of M1043, a monoclonal antibody targeting endoglin (ENG), in mitigating liver injury associated with NASH progression.

ENG, a coreceptor for transforming growth factor (TGF)-β, is implicated in various pathological processes, including fibrosis and angiogenesis. Elevated levels of soluble ENG (sENG) and transmembrane ENG are observed in NASH, suggesting its involvement in disease progression. Additionally, intracellular adhesion molecule-1 (ICAM-1) and vascular cellular adhesion molecule-1 (VCAM-1) play crucial roles in inflammation and endothelial dysfunction, key features of NASH.

In this study, male mice were divided into control, choline-deficient L-amino acid defined high fat diet (CDAA)+rat IgG, and CDAA+M1043 groups, with the latter two groups fed a CDAA-HFD inducing NASH changes. Mice were treated with M1043 for four weeks, and liver samples were analyzed for protein expression of ENG, ICAM-1, and VCAM-1. Results showed that CDAA-HFD induced liver injury, as evidenced by elevated liver enzymes, and upregulation of ENG, ICAM-1, and VCAM-1. Importantly, M1043 treatment significantly prevented CDAA-HFD induced increase in the expression of these markers, suggesting its potential therapeutic efficacy in NASH.

Our findings highlight the promising role of M1043 in mitigating liver injury associated with NAFLD. Further research is needed to elucidate the underlying mechanisms and evaluate the translational potential of M1043 as a therapeutic agent for liver diseases.

Abstrakt

Játra hrají ústřední roli v lidské fyziologii a jejich zranitelnost vůči metabolickým poruchám, jako je nealkoholická steatohepatitida (NASH), podtrhuje potřebu účinných terapeutických zásahů. Tato práce zkoumá potenciál M1043, monoklonální protilátky cílené na endoglin (ENG), při zmírňování poškození jater spojeného s progresí NASH.

ENG, je koreceptor pro transformující růstový faktor (TGF)-β, který se podílí na různých patologických procesech, včetně fibrózy a angiogeneze. U NASH jsou pozorovány zvýšené hladiny solubilního ENG (sENG) a transmembránového ENG, což naznačuje jeho zapojení do progrese onemocnění. Kromě toho hrají intracelulární adhezní molekula-1 (ICAM-1) a vaskulární adhezní molekula-1 (VCAM-1) klíčovou roli v zánětu a endotelové dysfunkci, což jsou klíčové rysy NASH.

V této studii byli myší samci rozděleni do kontrolní skupiny, skupiny (vysokotukové diety) CDAA+rat IgG a skupiny CDAA+M1043, přičemž poslední dvě skupiny byly krmeny CDAA-HFD vyvolávající změny NASH. Myši byly po dobu čtyř týdnů léčeny přípravkem M1043 a vzorky jater byly analyzovány na expresi proteinů ENG, ICAM-1 a VCAM-1.

Výsledky ukázaly, že CDAA-HFD vyvolala poškození jater, což se projevilo zvýšením jaterních enzymů a zvýšenou expresí ENG, ICAM-1 a VCAM-1. Důležité je, že podávání M1043 významně zabránila zvýšení exprese těchto markerů vyvolané CDAA-HFD dietou, což naznačuje jeho potenciální terapeutickou účinnost u NASH.

Naše zjištění zdůrazňují významnou úlohu M1043 při zmírňování jaterního poškození spojeného s NAFLD. K objasnění základních mechanismů a vyhodnocení translačního potenciálu M1043 jako terapeutického prostředku pro jaterní onemocnění je zapotřebí dalšího výzkumu.

Table of Contents

List of abbreviations

- NAFLD non-alcoholic fatty liver disease
- NASH non-alcoholic steatohepatitis
- HCC hepatocellular carcinoma
- ENG endoglin
- TGF transforming growth factor
- sENG soluble endoglin
- ICAM-1 intracellular adhesion molecule-1
- VCAM-1 vascular cellular adhesion molecule-1
- LSECs liver sinusoidal endothelial cells
- TRC105 carutoximab
- mAB monoclonal antibody
- PV portal vein
- HA hepatic artery
- CNS central nervous system
- VLDL very low-density lipoprotein
- GSH glutathione S-transferase
- CTLs cytotoxic T lymphocytes
- NK natural killer cells
- iNKT invariant natural killer T cells
- MAIT mucosal-associated invariant T cells
- DCs dendritic cells

- ILCs innate lymphoid cells
- ALT alanine aminotransferase
- AST aspartate aminotransferase
- CCL2 chemokine CC ligand-2
- TNF-α tumor necrosis factor-alpha
- IL-6 interleukin 6
- CRP C reactive protein
- FFA free fatty acid
- T2D type 2 diabetes
- MDBs Mallory-denk bodies
- MRI magnetic resonance imaging
- PDFF proton density fat fraction
- DAMPs damage-associated molecular pattern
- ATP adenosine triphosphate
- HPCs hepatic progenitor cells
- TLR toll like receptor
- ZP zona pellucida
- OD orphan domain
- ALK activin receptor-like kinase
- BMP bone morphogenic protein
- HHT hereditary hemorrhagic telangiectasia
- ECM extracellular matrix
- HCV hepatitis C virus

- LFA-1 lymphocyte function associated-1
- VEGF venous endothelial growth factor
- MCD methionine-choline deficient diet
- CD choline deficient
- HFD high fat diet
- CDE choline deficient ethionine supplemented
- DIAMOND diet-induced animal model of NAFLD
- CDAA choline-deficient L-amino acid-defined diet
- CCl4 carbon tetra chloride
- DEN diethylnitrosamine
- TAA thioacetamide
- STZ streptozotocin
- CD105 endoglin
- ADCC antibody-dependent cellular cytotoxicity
- BCA bicinchoninic acid assay
- HRP horseradish peroxidase
- Ctrl control group
- SDS sodium-dodecyl sulphate
- TEMED tetramethylethylenediamine
- APS ammonium persulphate
- GAPDH glyceraldehyde-3-phosphate dehydrogenase
- TBS tris buffer saline
- CAF cancer associated fibroblast

- SMAD small mothers against decapentaplegic

1. Introduction

The liver plays a vital role in physiology of human body. The increasing incidence of metabolic diseases, including obesity, dyslipidemia, and diabetes, can lead to various liver disorders such as non-alcoholic fatty liver disease (NAFLD). The presence of steatosis (excessive fat accumulation within hepatocytes), inflammation, and tissue fibrosis participate the development of non-alcoholic steatohepatitis (NASH), a condition with potential progression to cirrhosis and hepatocellular carcinoma (HCC). [1]

Endoglin (ENG), defined as a transforming growth factor (TGF)- β coreceptor, exists in two distinct forms: a transmembrane glycoprotein and a soluble form. It has a physiological function in endothelium and plays a crucial role in cell proliferation and angiogenesis. Some studies suggest that both soluble endoglin (sENG) and transmembrane ENG are overexpressed in NASH. On the other hand, elevated plasma levels of sENG stimulates liver activities, working to reduce cholesterol levels in the bloodstream by redistributing it from plasma to hepatocytes and subsequently to bile [2], [3], [4], [5].

Intracellular adhesion molecule-1 (ICAM-1), a glycoprotein placed on the cell surface and belonging to the immunoglobulin family, serves as a key mediator. In the case of inflammation, ICAM-1 effectively attracts leukocytes from the bloodstream. ICAM-1 is predominantly present on vascular endothelial cells, epithelium, and immune cells. Moreover, higher expression of ICAM-1 relates to the inflammatory response [6].

Vascular cellular adhesion molecule-1 (VCAM-1) is another cell adhesion molecule that belongs to immunoglobulin family. It is responsible for facilitating the adhesion of monocytes to liver sinusoidal endothelial cells (LSECs) in response to inflammation, making it as one of the pivotal proteins upregulated in NASH [7].

TRC105 (carutoximab) is a monoclonal antibody (mAb) specifically designed to blocks ENG and it is signaling pathway. TRC105 was originally developed with primary focus on targeting endothelial proliferation in solid tumors within the field of oncology [8].

TRC105 binds more selectively to human ENG and effectively inhibits its expression and signaling pathway. However, it has less affinity to mouse ENG and subsequently inhibits it notably lower, resulting in less significant inhibition.

Therefore, a mouse-specific ENG-targeting rat IgG1 antibody, named M1043, has been formulated for specific application in preclinical investigations [9].

This study principally investigated the impact of M1043 on the expression of three key proteins: ENG, ICAM-1, and VCAM-1, which serve as critical biomarkers for NASH.

2. Liver

2.1. Liver histology

The liver is the largest organ in the abdomen, is partitioned into four anatomical lobes based on peritoneal attachment. From the anterior view, the right and left lobe are separated by falciform ligament, while the caudate lobe and quadrate lobe are observable from the posteroinferior view. Typically, the liver exhibit three significant fissures and three smaller ones. Among the major fissures, which are not apparent on the surface, are the main portal fissure, right portal fissure and the left portal fissure. The three minor fissures, visible as distinct physical clefts on the liver surface, include the umbilical fissure or fissure for round ligament, the venous fissure or fissure for ligamentum venosum, and the sulcus of the caudate process [10].

The liver's blood perfusion is facilitated by two main vessels: the hepatic portal vein (PV) and the hepatic artery (HA). Deoxygenated blood rises through the portal vein, carrying digested nutrients from the gut, pancreas, and spleen. The portal vein provides approximately 80% of the

total blood perfusion to the liver. The remaining blood circulation to the liver is supplied by hepatic artery, providing fully oxygenated blood [11], see Figure 1 [12].

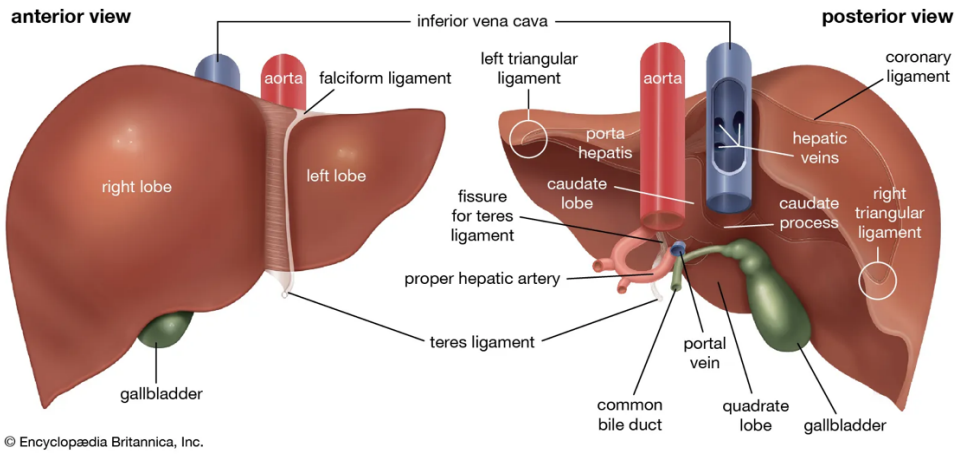

Figure P1: Liver anatomy with anterior and posterior views [12]

The first microscopic anatomy of the liver was explained in 1833 by Kiernan, who coined the term ’classic lobule’ or ‘Kiernan lobule’. The classic lobule was described as polygonal-shaped structures with a central vein and portal tracts located at the vertices, defining it as the basic histological unit of the liver. In 1954, Rappaport and colleagues introduced the ‘hepatic acinus’ model, as the next description of hepatic lobules. In this model, hepatic lobules are divided into three zones based on terminal portal circulation. With zone 3 being the nearest to the central veins. Another model, termed the Portal lobule’, situates the portal tracts at the center of lobules, see Figure 2 [13].

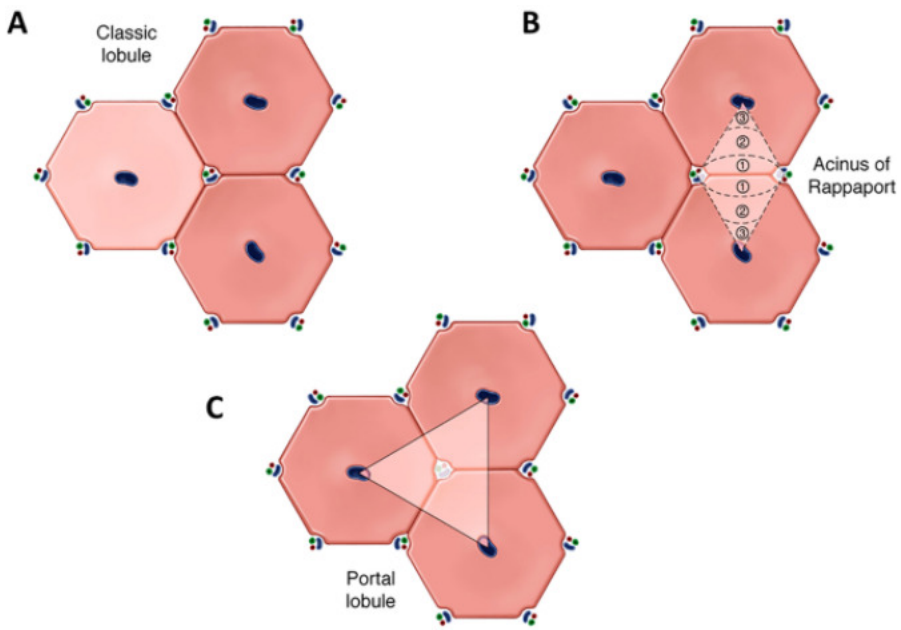

Figure 2: Different microscopic anatomies of liver [13]

2.1.1. Cellular anatomy

The cellular anatomy of the liver consists of various cell types, including hepatocytes, hepatic stellate cell, biliary epithelial cells (cholangiocytes), Kupffer cells and liver sinusoidal endothelial cells. Each population of cells perform distinct task that collectively contribute to the regulation of the hepatic function.

Hepatocytes are the primary epithelial cells in the liver, are responsible for various metabolic functions. It is widely recognized that hepatocytes can undergo infinite regeneration, a crucial attribute that proves beneficial in liver transplantation and surgical resection.

Cholangiocytes, constituting the second most prevalent epithelial cells in liver, contribute to the formation of the bile duct lumen. Hepatic stellate cells are responsible for storing vitamin A in lipid droplets. However, certain liver injuries can activate stellate cells, leading to proliferation and gradual loss of vitamin A stores. Another function of stellate cells is the deposition of collagen

in the liver in response to hepatic injury, resulting in the formation of scar in liver tissue that may progress to liver cirrhosis.

Kupffer cells play a role in immune responses within the liver and act as phagocytic cells, functioning as resident macrophages. The final group, liver sinusoidal cells, comprises specific endothelial cells that form porous sieve plates within the sinusoidal lumen. They play a crucial role in certain protein transfers between plasma and liver cells [14], [15].

2.2. Liver function

The liver is involved in a series of critical physiological processes in the body. Its most important function is metabolism, encompassing the processing of macronutrients and xenobiotics, playing a significant role in both. Additionally, the liver is responsible for regulating blood volume, endocrine regulating of growth signaling pathways, supporting immune system, and maintaining lipid and cholesterol homeostasis [14].

Moreover, in recent years, the liver's response to both nutrient overabundance and deficit has been observed. This response involves the secretion hepatokines, acting as signals for energy status, and regulating nutrition to peripheral tissue and the central nervous system (CNS). The liver primarily regulates systemic glucose hemostasis by controlling glucose production or glycogen storage. Its uptakes excess glucose from the plasma, storing it in the form of glycogen or even consuming it for lipogenesis. This response occurs in reaction to elevated blood glucose levels and insulin, typically after a meal. During this state, hepatic glucose formation also decreases. On the contrary, glycogenolysis and gluconeogenesis play significant roles during fasting or periods of low carbohydrate intake. Additionally, the liver engages in the oxidation of lipids to forms ketones

and provides lipids in the form of very low-density lipoprotein (VLDL) to peripheral tissues. Any imbalance in these diverse pathways may lead to insulin resistance or fatty liver disease [16].

The liver plays a crucial role in detoxifying harmful substances, known xenobiotics through process is called metabolism. Metabolism mainly involves two phases. The first phase is predominantly carried out by cytochrome p450 superfamily, with enzymes such as CYP3A4, CYP2D6 and CYP2C9. These enzymes facilitate pathways such as oxidation, reduction, and hydroxylation, introducing an oxygen atom into the substrate to form a more polar metabolite. This modification readies the substrate for the second phase of metabolism. The second phase of metabolism, known as conjugation, involves the addition of a hydrophilic molecule to the substrate, making it more readily extractable. Enzymes involved in phase two metabolism include UDP-glucuronyltransferase, glutathione S-transferase (GSH), sulphotransferase, N-acetyltransferase and methyltransferase [17], [18].

Bile production is yet another principal function of the liver, essential for the digestion and absorption of fats and hydrophobic substances in the small intestine [19]. Bile is mainly consisting of water, which dissolves various substances including bile acids, bilirubin, phospholipid, and cholesterol. Bile acids, the main principal component of bile, are responsible for emulsifying dietary lipids and are generated from cholesterol by hepatocytes. The gallbladder is the organ where bile concentrates before delivering directly to the small intestine [20], [21].

The hepatic immune microenvironment contains abundant cells from both the innate and adaptive immune systems, working to maintain tolerance in a hemostatic form. These immune cells play a role in initiating inflammation and causing liver injury during times of disease. Adaptive immune cells include regulatory T cells, cytotoxic T lymphocytes (CTLs) and various helper T cell subsets such as Th1, Th2, Th17 and Th22. Additionally, B cells and plasma cell

populations contribute to the complex immune milieu in the liver. Innate immune system includes cells identified as liver resident, such as Kupffer cells, along with natural killer (NK) cells, invariant NKT (iNKT) cells, mucosal-associated invariant T (MAIT) cells, dendritic cells (DCs), γδ T cells, and innate lymphoid cells (ILCs). [22]

In brief, the liver serves as a primary immune organ, particularly with its resident phagocytic cells that identify and eliminate potential pathogens from the blood circulation. The key to a healthy liver function lies in the balance between hepatic immune hypo-responsiveness against typical levels of microbe-derived molecules and strong inflammatory response to the shift in the quantity or context of microbial products [23].

3. Non-alcoholic steatohepatitis (NASH)

3.1.1. Pathophysiology

Non-alcoholic steatohepatitis (NASH) is a chronic liver disease and represents an advanced stages of non-alcoholic fatty liver disease (NAFLD). The primary cause of chronic liver disease is the accumulation of excessive fat in the hepatocytes, influenced by factors such as genetics, unhealthy diet, sedentary lifestyle, obesity, and metabolic diseases. NASH is characterized by inflammation and hepatocytes injury in conjugation with hepatic steatosis. Specific indicators, including biochemical markers and factors related to inflammation or fibrosis, are associated with NASH.

Biochemical markers such as alanine aminotransferase (ALT) and aspartate aminotransferase (AST), measurable in plasma or liver tissue, serve as indicators of non-specific hepatocyte damage. Elevated levels of ALT, two to four times the normal may signify NASH. High levels of triglyceride or cholesterol, measured in plasma or liver biopsy, can also be related to NASH. Additionally inflammatory cytokines and chemokines, such as interleukin 6 (IL-6), tumor

necrosis factor-alpha (TNFα), chemokine CC ligand-2 (CCL2), and C reactive protein (CRP), are significant markers of NASH [24].

Insulin resistance in the liver, muscle, and adipose tissue is closely associated with NAFLD or NASH, often accompanied by the presence of hyperinsulinemia. Interestingly, hyperinsulinemia has been documented in individuals without obesity but with normal glucose tolerance. A study has elucidated that individual with NAFLD or NASH exhibit insulin resistance (elevated production of endogenous glucose and free fatty acid (FFA) release) in both hepatic and adipose tissue. This insulin resistance persists even in hyperinsulinemia condition, distinguishing it from individuals without liver diseases. A recent meta-analysis revealed that among individuals with type 2 diabetes (T2D), the occurrence rate of NASH is 37.3% [25].

3.1.2. Histological description of NASH liver

In general, there is a subtle distinction in the histological features between NAFLD and alcohol induced liver injury. The histopathological description of NASH includes several key features, including predominantly macrovesicular steatosis, scattered inflammation and apoptotic bodies, ballooning degeneration of hepatocytes, and the presence of Mallory-Denk bodies (MDBs) [26].

NASH represents the predominant histologically advanced stage of NAFLD and is nearly always associated with some degree of fibrosis. In comparison to other forms of steatosis alone, NASH commonly exhibits mild portal inflammation and a mild ductular reaction. Uncommon characteristics in NASH include the occurrence of lymphoid aggregates, resembling hepatitis C, a high number of plasma cells as observed in autoimmune hepatitis, and bile duct injury

characteristic of primary biliary cirrhosis. Despite surgical or pharmacological interventions for NASH portal inflammation might persist or escalate, even when steatohepatitis resolves [27].

3.1.3. Clinical manifestation

NASH is predominantly asymptomatic disease, and symptoms may become apparent only as it progresses to cirrhosis and hepatocellular carcinoma. Typically, NASH is discovered during routine health check-ups, often coinciding with conditions such as obesity, dyslipidemia, diabetes, and insulin resistance, collectively known as metabolic syndrome. The diagnosis of NAFLD/NASH relies on three main criteria: the absence of excessive alcohol consumption, the detection of steatosis through imaging or histology, and the proper exclusion of alternative liver diseases. NASH diagnosis is established by the presence of steatohepatitis as confirmed through liver biopsy, which is currently considered the gold standard [28]. liver biopsy, in addition to being costly, is an invasive procedure associated with significant sampling error and potential complications such as pain, bleeding, and, in rare cases, death. Due to the limited acceptance of this invasive procedure by patients, there is a growing demand for precise and non- or minimally invasive biomarkers. Liver enzymes alone are not reliable indicators, despite the common occurrence of abnormal levels in patients with NAFLD. It should be noted that individuals with advanced liver diseases such as cirrhosis or HCC, may present decreased levels of aminotransferases.

An alternative predictor is Magnetic Resonance Imaging (MRI), which measures the proton density fat fraction (PDFF) and serves as a precise and quantitative indicator of hepatic fat content [29].

3.2. Liver fibrosis in NAFLD

Generally, in most patients with NAFLD, the disease may progress slowly and is more stable. In rare cases, it can develop into cirrhosis and hepatocellular carcinoma (figure 3). These end-stage liver diseases include advanced levels of tissue fibrosis, which can bring about more complications. Fibrosis can develop in either NAFLD or NASH, but it progresses more rapidly in individuals with NASH, triggered by necroinflammation. The histological grading system, which clarifies the staging of fibrosis, spans from stage 0 (absence of fibrosis) to stage 4 (cirrhosis). A meta-analysis of studies on NAFLD, which evaluated paired liver biopsy samples, discovered that fibrosis progression increased by one stage over 14.3 years for those with NAFLD and by one stage over a period of 7.1 years for individuals with NASH [30].

From a molecular perspective, NASH involves inflammation that leads to the death and apoptosis of the hepatocytes. Damage-associated molecular pattern (DAMPs) issues from the dying hepatocytes, containing nucleic acid, intracellular proteins, and adenosine triphosphate (ATP), which act as damaging signals to neighboring cells. In response, these signals activate hepatic progenitor cells (HPCs). In contrast, apoptosis yields lower levels of DAMPS. These apoptotic bodies are subsequently engulfed by hepatic stellate cells (HSCs) and Kupffer cells, initiating a pro-fibrogenic response. Furthermore, the DNA derived from apoptotic hepatocytes triggers the activation of Toll-Like-Receptor (TLR)-9 on HSCs, leading to collagen production [31].

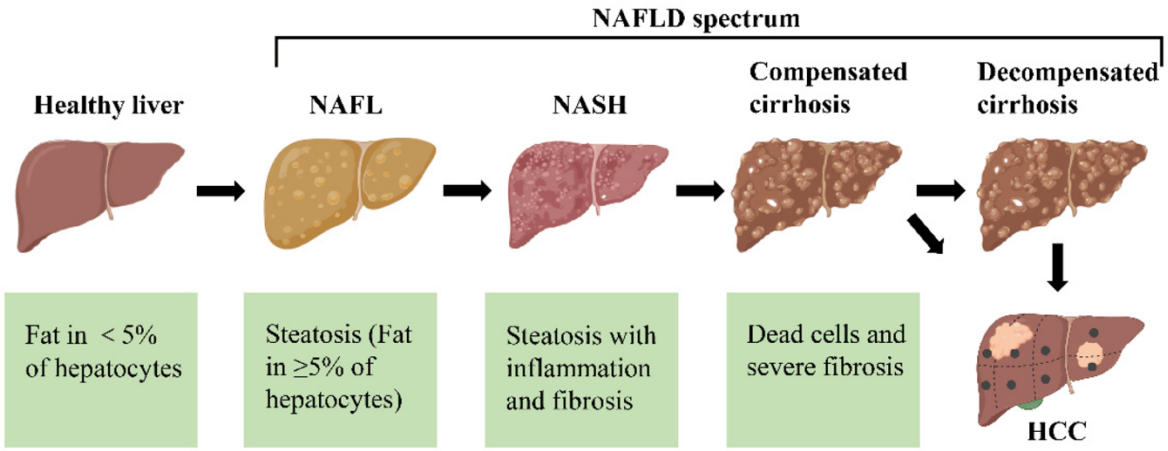

Figure 3: Stages of NAFLD progress [32]

4. Endoglin

4.1. Structure and function

Endoglin, also known as ENG or CD105, is a type 1 transmembrane glycoprotein, a homodimer held together by disulfide linkages, consisting of two 90 kDa subunits which make a 180 kDa molecule. It is recognized as a co-receptor for ligands belonging to the Transforming Growth Factor β (TGF-β) superfamily. The main structural features of ENG include a 561-residue extracellular domain and a 47-residue serine/threonine-rich cytoplasmic region. A conserved region of the extracellular residue is called zona pellucida (ZP), and at its N-terminal extracellular region, a domain of unknown function lacking homology to any other identified protein is consequently referred to as the Orphan domain (OD) [4], [33], [34].

ENG comprises a cytoplasmic domain and has been identified with two distinct protein variants. The primary isoform is short endoglin (S-ENG), consisting of 17 amino acids, and long endoglin (L-ENG), comprising 47 amino acids [35]. These variants differ in their promotion of two

distinct pathways, L-ENG enhance ALK-1ld1 pathway, while S-ENG stimulate ALK-5-PAl pathway [36]. It also exists in another two different isoforms; transmembrane ENG express on different cells and soluble endoglin (sENG) circulating in blood stream.

In the case of membrane-bound ENG, it has been discussed that the extracellular region interacts with types I and II TGF-β ligands, activin receptor-like kinase (ALK)1, (ALK)-5, Bone Morphogenic protein (BMP-9) and (BMP-10), which are members of the TGF-β family [33], [37] . ENG plays a role in both physiological functions and certain pathological conditions.

Various cells type express ENG, including endothelial cells, vascular smooth muscles, hepatic stellate cells, activated monocytes, macrophages, and fibroblasts. The overexpression of ENG is observed in proliferating endothelial cells and within the vascular endothelium of tumor tissues [4], [38], [39].

Physiologically, ENG is involved in cardiovascular development, homeostasis, angiogenesis, and vascular remodeling. A pathologic condition known as Hereditary Hemorrhagic Telangiectasia (HHT) can develop due to mutation in the human *ENG* gene. This condition is characterized by symptoms such as nosebleeds, gastrointestinal bleeding, arteriovenous malformation in the liver, lung, brain, as well as manifestation of telangiectasis on skin and mucosa. On the other hand, elevated expression of sENG in the plasma may serve as an indicator of preeclampsia, a metabolic disorder occurring during pregnancy [33].

4.2. ENG role in liver disorders

Transforming growth factor (TGF-β) serves as a pivotal cytokine with diverse regulatory functions in both developmental and physiological homeostasis. It regulates cellular proliferation, differentiation, and the synthesis of extracellular matrix (ECM). Notably, TGF-β stand out as a

potent profibrotic cytokine, and the manifestation of aberrant TGF-β signaling is conspicuously linked to various fibrotic conditions [40].

ENG, has been found to impact development and progression of fibrosis through heightened expression in cells that promote fibrotic processes, such as mesangial cells, scleroderma fibroblasts, and hepatic stellate cells [40], [41].

Remarkably, despite hepatic stellate cells being recognized as the most fibrogenic cell type in the liver, investigations have consistently revealed elevated levels of soluble ENG in the bloodstream during liver fibrosis. This observation suggests the possibility of increased ENG expression and subsequent release of its ectodomain from liver cells in the context of liver fibrosis. In many carcinomas endoglin is a major biomarker of angiogenesis, involving HCC. The higher expression of endoglin in endothelial cells of small vascular and lymphatic vessels has been seen in HCC as well as other cancer tissues [42].

The role of ENG in carcinogenesis exhibits variability contingent upon the specific tumor type and cellular origin of endoglin production (vascular endothelial cells or tumor cells). This protein assumes a dualistic role, either promoting tumor growth and progression or inhibiting tumor development and acting as a suppressor. Elevated ENG expression in tumor endothelial cells is associated with increased tumor growth, indicating a pro-angiogenic role. On the contrary, its downregulation is linked to reduced tumor angiogenesis and diminished tumor growth. Moreover, higher ENG expression in tumor cells is correlated with tumor suppression, while reduced ENG levels contribute to tumor progression, facilitating migration, invasion, and malignancy [42].

Some studies suggest that ENG is also involved in Hepatitis C Virus (HCV) related liver fibrogenesis. These studies identified a heightened prevalence of rare variants in the *ENG* gene among individuals exhibiting fibrosis [43].

5. Cell adhesion molecules in liver disorders

5.1. ICAM-1

It was demonstrated that there are different cell adhesion molecules participating in liver diseases. Intercellular Adhesion Molecule-1 (ICAM-1) is a transmembrane glycoprotein known for attracting leucocytes from the blood circulation in case of an inflammation. While the major site for ICAM-1 expression is on the vascular endothelial cells, it can be also expressed on epithelial cells, hepatocytes, fibroblasts, and hematopoietic cells. The highest expression occurs during inflammation on epithelial and immune cells, triggered by proinflammatory cytokines, including interferon gamma, IL-1, and TNF-a [44], [45]. The interaction between ICAM-1 and its ligand, lymphocyte function accociated-1 (LFA-1), member of CD18 family of adhesion molecules, promotes leukocytes and immune cells infiltration and adhesion [46].

A study suggests that increased levels of ICAM-1 are strongly associated with an elevated risk of NAFLD development, and this inflammatory mediator can serve as one of the major biomarkers for the prediction of NAFLD [47]. On the other hand, another study found that ICAM-1 can influence hepatocyte proliferation. They explained that the bond between ICAM-1 and leukocytes can stimulate hepatocyte regeneration after hepatectomy through release of TNF-alpha and IL-6 by Kupffer cells [48]. It's evident that inflammation can boosts tumor growth and metastasis, representing a distinct feature of cancer progression. Soluble ICAM-1 triggers the tumor cells to release proangiogenic vascular endothelial growth factors (VEGF) and can also causes the tumor cells to express higher amounts of pro-metastatic genes, in inflammation, HSCs

may differentiate into myofibroblasts. These myofibroblasts promote desmoplasia and a proangiogenic stroma, forming the early state of micrometastasis through secretion of VEGF and metalloproteinases [46].

In summary, a study explained that serum ICAM-1 levels are higher in the following order: 1. alcoholic steatohepatitis, 2. NASH, 3 NAFLD. The study also mentioned that the presence of high blood pressure together with NAFLD causes higher levels of serum ICAM-1 compared to cases without high blood pressure [45].

5.2. VCAM-1

Vascular Cell Adhesion Molecule-1 (VCAM-1) is an adhesion molecule mostly expressed on endothelial cells, playing a significant role in liver disorders, particularly NASH and liver fibrosis. Its upregulation is triggered by inflammatory stimulation. VCAM-1 activates the endothelial signaling pathway through NADPH oxidase-generated reactive oxygen species, creating pathways between cells for the migration of leukocytes [49].

The elevated expression of VCAM-1 contributes to the adherence and extravasation of circulating monocytes to vessels, promoting to hepatic injury, inflammation, and fibrosis [50]. It has been established that VCAM-1 is overexpressed in patients with NASH compared to normal liver or fatty livers of NAFLD patients [50]. This makes it a potential biomarker of endothelial dysfunction and angiogenesis, capable of distinguishing different NAFLD disease stages [51].

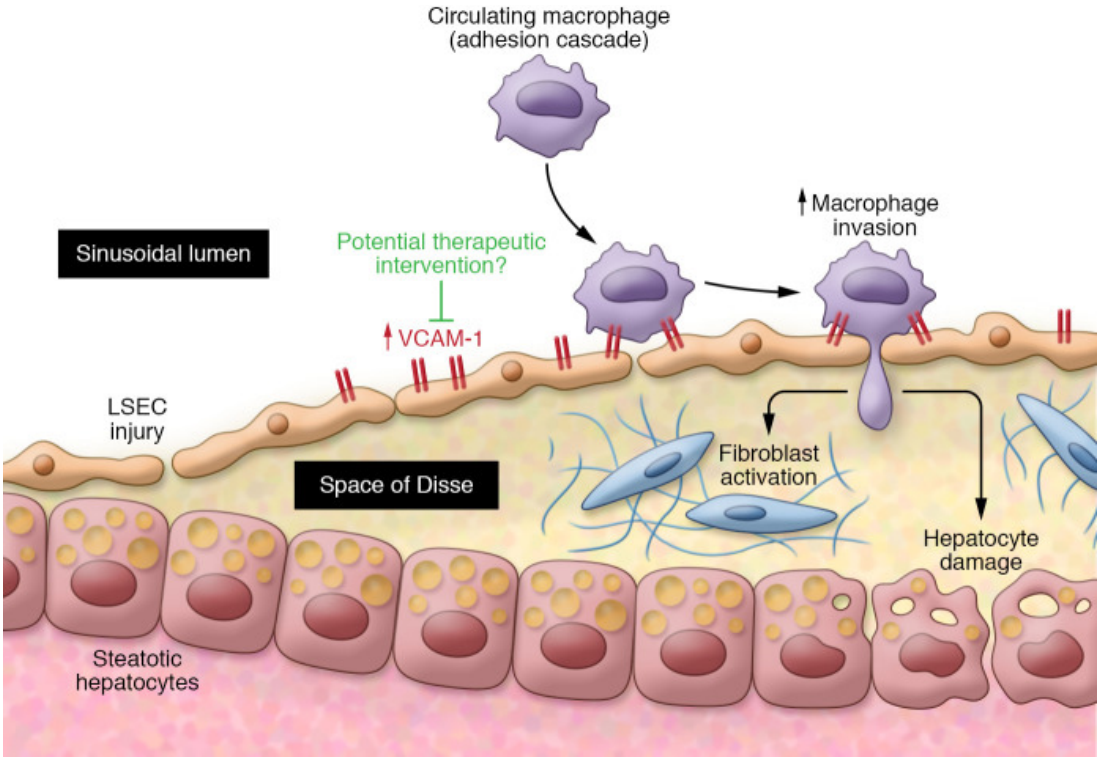

Figure 4: VCAM-1 expression on endothelial cells adheres circulating macrophages [50]

Blocking VCAM-1 has been associated with decreased expression, a lower number of infiltrating macrophages, and diminished fibrosis in models NASH. Furthermore, there is a suggestion to use molecular imaging with an anti-VCAM-1 nanobody as a non-invasive method for identifying liver inflammation in cases of chronic liver disease. These results indicate that VCAM-1 could be a promising target for the development of treatments for liver disorders [52].

Recently, a study investigated that patient with COVID-19 also present increased serum levels of VCAM-1, which may clarify the systemic vascular inflammation that occurs to infected patients [53].

6. Liver sinusoidal endothelial cells dysfunction

Liver sinusoidal endothelial cells (LSECs) are specialized endothelial cells that serve as a crucial boundary between blood cells and hepatocytes/hepatic stellate cells. They form a permeable barrier characterized by fenestrae, the absence of a diaphragm, and the lack of a basement membrane, rendering them the most permeable endothelial cells in mammals [54].

LSECs play critical roles in preserving liver homeostasis by regulating vascular tone, inflammation, thrombosis, and orchestrating the hepatic immune response. However, during acute or chronic liver injury, LSECs alter their characteristics, impacting neighboring cells and contributing to the pathophysiology of liver diseases [55]. They undergo capillarization, leading to a loss of their protective functions, while also stimulating angiogenesis and vasoconstriction.

The process known as capillarization of LSECs, or dedifferentiation, takes place in response to liver injury, observed both in animal models and patients. This transition occurs early in the injury process, preceding the activation of hepatic stellate cells and macrophages, as well as the onset of liver fibrosis. These findings suggest that capillarization may represent a crucial initial stage required for the development of fibrogenesis [54].

LSECs contributes to impaired hepatic lipid uptake and metabolism, interrupted transport of macromolecules and metabolites, increased angiogenesis, intrahepatic inflammation, hepatocellular injury, and ultimately, diminished hepatic blood flow accompanied by intrahepatic resistance [56].

7. NASH animal models

A suitable preclinical model for NAFLD should accurately replicate the underlying mechanisms of the human disease, particularly in its advanced stages. A clinically relevant mouse model should exhibit typical histopathological characteristics of NASH, including steatosis, inflammation, ballooning, and some level of liver fibrosis. These animal models encompass genetically induced, diet-induced, and chemical-induced NASH models.

7.1. Diet-induced models

In dietary models, the methionine-choline deficient (MCD) diet is one of the best-known diets for NAFLD development, involving 40% sucrose and 10% fat content. Choline and methionine are two essential nutrients, and their deficiency causes reduced β-oxidation and alter the formation of very low-density lipoprotein (VLDL), resulting in excessive fat accumulation in the liver, hepatocytic cells death, oxidative stress, and release of differentiating cytokines with modest levels of inflammation and fibrosis [57]. Choline deficient (CD) diet itself also used in fatty liver disease studies often features elevated fat levels, which can lead to steatosis, inflammation, and fibrosis. Unlike MCD diets, CD diets do not typically result in weight loss, making them preferable to certain researchers. Another diet, the fructose diet, can also cause the development of NAFLD as it is primarily metabolized by the liver. This can trigger excessive fat deposition and inflammation, leading to insulin resistance and fibrosis in hepatic tissue. A high fat diet (HFD) comprises a regimen with 45 to 75 kcal% fat content and represents human disease such as obesity, insulin resistance and hyperlipidemia. This diet leads to accumulation of triglycerides in the liver, resulting in the development of NASH [57].

Some other examples of dietary models include the choline deficient-ethionine supplemented (CDE) diet, American lifestyle-induced obesity syndrome (ALIOS) diet, and the Diet-induced animal model of NAFLD (DIAMOND) [58].

7.1.1. CDAA animal model description

The CDAA diet, or choline-deficient L-amino acid-defined diet, is used for inducing NASH in rodent animals Similar to the MCD diet, the CDAA diet differs only in the proteins which are replaced with an equivalent and related mixture of L- amino acids. It functions by inhibiting fatty acid oxidation in liver cells, leading to increased lipid synthesis, oxidative stress, and inflammation, ultimately resulting in liver tissue fibrosis. The CDAA diet takes more time to induce histopathological changes compared to the MCD diet. Mice following the CDAA diet show no signs of hepatic insulin resistance, do not experience weight gain or alterations in peripheral insulin sensitivity. This model has been demonstrated to replicate human NASH in both mice and rats, inducing steatohepatitis, liver fibrosis, and hepatocellular carcinoma sequentially [59], [60].

On the other hand, the CDAA diet combined with high-fat diet (CDAA-HFD) causes weight gain and elicit features of the metabolic syndrome, as well as rapid development of NAFLD. Compared to the CDAA diet alone, CDAA-HFD exhibits a closer resemblance to the pathology of NASH in humans [58].

7.2. Chemically induced models

In chemical-induced models, carbon tetra chloride (CCl4) can be mentioned, causing hepatic damage characterized by degenerated, ballooned, and necrotic hepatocytes. CCl4 itself induces fibrosis, but without obesity or insulin resistance. To use it as NASH model, it needs to be combined with high fat diet (HFD). Diethylnitrosamine (DEN) is a recognized carcinogen, suitable for creating HCC animal model or studying HCC progression in NAFLD [57], [61]. Thioacetamide (TAA), when combined with fast-food diet, can also lead to development of NASH [58]. Streptozotocin (STZ) is another chemotoxin to pancreatic beta cells, causing a gradual loss in insulin formation. However, it also leads to hepatotoxicity independent from hyperglycemia [62].

7.3. Genetically induced models

Genetically modified models can be combined with appropriate interventions, such as a specific diet and become a valuable tool for studying the pathogenesis of NASH and evaluating potential therapeutic interventions. ob/ob mice carry a mutation that leads to leptin deficiency, resulting in obesity and metabolic dysfunction. The application of high-fat diet to these mice can induce NASH for further studies. The db/db mouse present another kind of mutation in the gene encoding the leptin receptor. Depending on their diet, these mice may develop micro- and macrovesicular hepatic steatosis along with necroinflammation. Additional examples include foz/foz mice, fatty liver shionogi mice, PNPLA3 polymorphism (patatin-like phospholipase domain-containing 3), and *Gankyrin* (*Gank*)-Deficient Mice [58], [62].

8. Anti-endoglin antibodies

Anti-ENG antibodies have been studied for their effectiveness in suppressing metastasis and primary tumors by targeting tumor vasculature. Nowadays, antiangiogenic therapies are gaining more attention due to their advantages over conventional tumor-cell targeted treatments, such as chemotherapy or immunotherapy. These advantages may include overcoming issues like drug resistance, poor delivery, and tumor heterogeneity [61], [63].

8.1. Carotuximab (TRC105)

Carotuximab, also known as TRC105, is a chimeric human IgG1 antibody designed to target ENG expression and signaling [64]. Given that ENG is crucial in angiogenesis and is upregulated in hypoxia, TRC105 was shown to be effective in inhibiting angiogenesis. The angiogenesis inhibition mechanism involves TRC105 competitively inhibiting the activating ligand of ENG, namely bone morphogenic protein (BMP), and facilitating antibody-dependent cellular cytotoxicity (ADCC). TRC105 exhibits its effects through diverse mechanisms. Initially, its binding to ENG triggers ADCC, facilitated by NK cells, neutrophils, and monocytes, leading to the destruction of target cells. Secondly, TRC105 prevents the binding of BMP-9 to ENG, inhibiting the formation of the receptor complex and impeding ENG-mediated downstream signaling. Lastly, TRC105 induces MMP-14-mediated shedding of ENG, resulting in the generation of sENG. This soluble form acts as a ligand trap, reducing ENG signaling in the process [65].

Some preclinical studies suggest that targeting both ENG and Vascular Endothelial Growth Factor (VEGF) pathways together may lead to better inhibition of angiogenesis compared to targeting them individually [66], [67].

The efficacy of TRC105 was demonstrated in mice deficient in Fc gamma receptors I-IV, which are incapable of inducing ADCC [65]. The research revealed that TRC105 specifically targets a subset of intratumoral regulatory T cells expressing ENG, effectively eliminating this immunosuppressive population from the tumor microenvironment. These findings suggest that TRC105's targeting ENG plays a significant role in the regulation of immune effector cells [65], [35]. Inhibition of ENG by carotuximab promotes a protentional therapy in HCC treatment either as a solo therapy or combination with another anti-angiogenic medicine. However, further investigations are needed in the future [67]. TRC105 underwent phase 1 and 2 clinical trials involving patients with prostate, ovarian, bladder, breast, hepatocellular, and urothelial cancers, demonstrating minimal side effects. Recently, it has undergone investigation in a Phase 3 trial involved patients with angiosarcoma [68].

8.2. M1043

TRC105 not only prevents BMP-9 signaling through ENG but also engages mechanisms dependent on the immune system. Despite demonstrating clear anti-tumor effects in syngeneic mouse models, TRC105 exhibits significantly lower binding affinity for mouse ENG compared to human ENG. To better investigate the role of ENG-dependent BMP-9 signaling in preclinical models, researchers developed a mouse ENG-targeting antibody named M1043. Both TRC105 and M1043 effectively block BMP-9-induced SMAD1/5 phosphorylation in human and mouse endothelial cells, respectively, while leaving TGF-β-induced, ALK-5-dependent SMAD2/3 phosphorylation unaffected [69].

Additional experiments revealed increased basal SMAD2/3 phosphorylation and decreased SMAD1/5 phosphorylation in HUVECs upon TRC105 treatment [65], [70]. Although M1043

exhibits stronger inhibition of BMP-9 binding to mouse ENG compared to human ENG, it appears to be less potent than TRC105 in certain *in vivo* colorectal cancer models. The absence of ADCC induction in mice by the IgG subtype of M1043 (rat IgG1) further supports the notion that ADCC plays a crucial role in the therapeutic effects of the precise molecular mechanism through, which TRC105 disrupts BMP-9 binding was recently elucidated with the publication of the crystal structure of the human ENG ectodomain and its complex with the ligand BMP-9. BMP-9 interacts with a hydrophobic surface on the N-terminal orphan domain of ENG, involving residues mutated in HHT patients and overlapping with the TRC105 binding site [65].

9. Western blot analysis

9.1. The principle of the method

Western blot is a method that separates proteins via gel electrophoresis, followed by their transfer to a membrane and subsequent, immunodetection using specific antibodies against target antigen. It is an important technique for analysis of proteins, relying on the specificity of antibody-antigen interaction.

This method is commonly employed for qualitative or semi-quantitative detection of specific proteins and their respective molecular weights within a complex protein mixture [71], see Figure 5 [72].

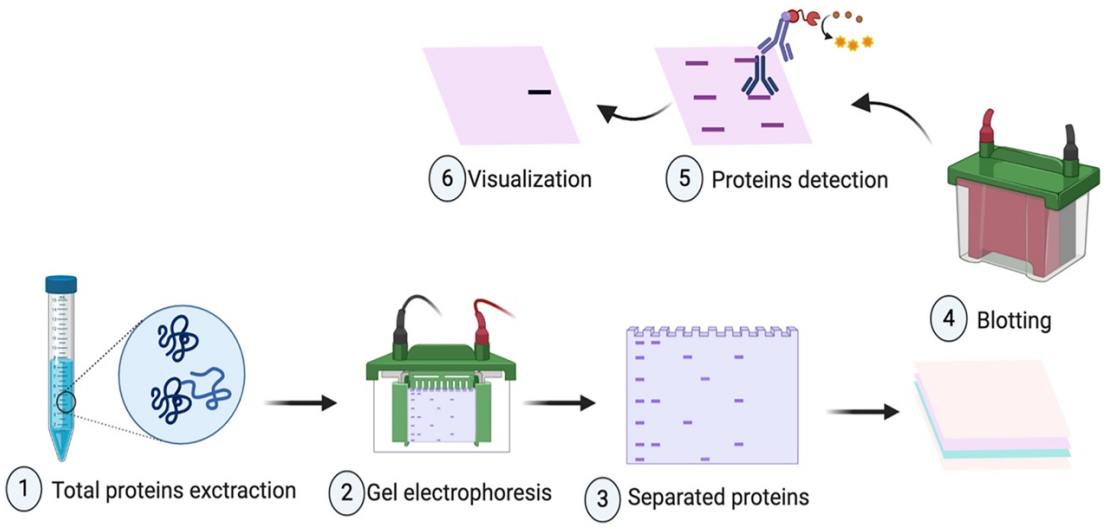

Figure 5: Steps of western blot laboratory technique [72]

Sample preparation: the first step is sample preparation, which is important to be done sensibly since the extraction and purification of proteins have a major impact on the results. Liquid nitrogen is used to freeze samples, which are then kept at -80° C for lysing. Mechanical homogenization is mainly used for cell and tissue lysis and disruption of cell membrane. To avoid

protein denaturation, homogenization is carried out at 4 C with a specific buffer containing protease inhibitor. The proteins we are searching for are in various cellular components such as the cell membrane, mitochondria, and the nucleus. It is crucial to determine the protein concentration of the samples following protein extraction, as this step is highly important for accurately calculating the specific amount of protein mass to be applied to each well in the gel. The Bicinchoninic acid assay (BCA) is the biochemical method employed to quantify the overall protein quantity in a solution. Bicinchoninic acid, upon the reduction of Cu+2 to Cu+1 in an alkaline solution, produces a purple color. This reduction is facilitated by the four amino acids in the protein: cysteine, cystine, tyrosine, and tryptophan. This process is significant in minimizing variations in the protein composition[73]. After measuring protein concentration, samples are diluted with Mili-Q water, sample buffer is added for electrophoresis visibility, and samples are heated to 95°C for protein denaturation.

Gel electrophoresis: western blotting employs two types of agarose gel: stacking and separating. The stacking gel, slightly acidic a pH of 6.8, has lower acrylamide concentration, creating a porous gel to distinct band formation. In contrast, the separating gel, with a basic pH 8.8 and higher polyacrylamide content, effectively separates proteins based on size, allowing smaller proteins to move more rapidly than larger ones. Proteins, loaded with a negative charge due to denaturation, migrate towards the positive electrode under applied voltage. Gels are typically formed between glass or plastic plates according to the described protocol. Samples and a marker are loaded into wells, while empty wells receive sample buffer. Careful voltage control is crucial during electrophoresis to prevent overheating and distortion of protein bands [73].

Blotting: After separating the protein mixture, an electric field perpendicular to the gel's surface transfers proteins to a membrane. The membrane is sandwiched between the gel and the

positive electrode, with fiber pads and filter papers for protection (figure 6). Key considerations include ensuring close contact between the gel and membrane for a clear image and proper placement of the membrane to facilitate the migration of negatively charged proteins. This electrophoretic transfer, whether conducted in wet or semi-dry conditions, is more reliable when performed wet, especially for larger proteins. The membrane, a crucial component, comes in two types: nitrocellulose, which has high protein affinity but is brittles, and PVDF, which offers better mechanical support for reprobing and storage. However, careful washing is essential due to higher background in PVDF membranes [73].

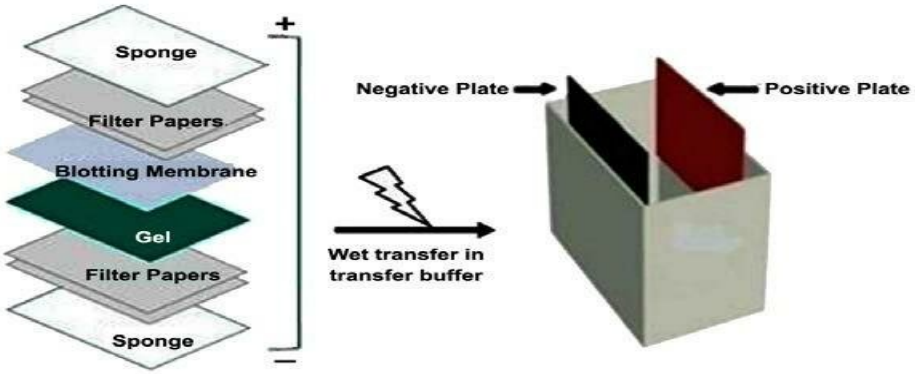

Figure 6: Formation of a sandwich in western blot [74].

Blocking and antibody incubation: Blocking is a critical step in western blotting, essential for preventing non-specific antibody binding to the membrane. Typically, a solution of 5% BSA or nonfat dried milk diluted in TBST is used for blocking to minimize background interference. primary antibody incubation often involves using BSA, as it is required in larger quantities compared to the secondary antibody, allowing for potential antibody reuse if needed. The concentration of the antibody is determined based on the manufacturer's instructions and can be diluted in a wash buffer like PBS or TBST. Effective washing is crucial to minimize background

and remove unbound antibody, but excessive washing should be avoided to prevent signal reduction. Following washing, the membrane is incubated with a labeled antibody, commonly using an enzyme such as horseradish peroxidase (HRP). The signal produced by HRP corresponds to the position of the target protein and is captured on a film, typically developed in a darkroom.

Chemiluminescence detection: in the final stage, Chemiluminescence is utilized for detection, typically within a device called ChemiDoc. ChemiDoc is an imaging apparatus equipped with a high-resolution system for imaging and quantifying gels and blots. After adding the chemiluminescent reagent onto the membrane, HRP catalyzes the substrate, resulting in a detectable colored signal. While the data acquired does not provide absolute protein quantity, it enables a relative comparison between samples. Consequently, Western blotting is a widely used for comparing the expression of specific proteins across various cells and tissues.

10. Aims of the diploma thesis

In this diploma thesis, we hypothesized that M1043 affect LSED by modulating the protein expression of ENG, VCAM-1 and ICAM-1 in a NASH mouse model induced by the CDAA-HFD. We aimed to evaluate the expression of ENG, ICAM-1, and VCAM-1 liver (sinusoidal endothelial cells) in the liver during the development and progression of NASH and after pharmacological intervention by western blot method.

11. Experimental part

11.1. Experimental animals

Fifteen male mice, aged 11-12 weeks, were used in this study and divided into three groups: the control group (Ctrl) (n = 5), the CDAA+rat IgGgroup (CD+IgG) (n = 5), and the CDAA+M1043 group (CD+M1043) (n = 5). The control group was fed with a standard chow diet (1314-10 mm pellets, Altromin, Germany), while the CD+IgG and CD+M1043 groups were fed with a CDAA-HFD (A06071302, Research Diets, USA) to induce NASH development.

After a 4-week period, which was previously confirmed to induce NASH development, the CD+IgG and CD+M1043 groups received intraperitoneal injections of rat IgG (10 mg/kg) and M1043 (10 mg/kg) respectively, twice a week. The experimental period lasted eight weeks, after that the mice were euthanized using an anaesthetic overdose induced by a combination of xylazine (10 mg/kg, i.p.) and ketamine (100 mg/kg, i.p.). Blood and liver samples were collected for further analysis. Liver samples were immediately frozen in liquid nitrogen, and stored at -80 °C until subsequent analysis, mainly for western blot analysis.

The mice were purchased from Velaz company (Prague, Czech Republic) and adapted for two weeks before the study. Throughout the experimental period, the animals were housed in a temperature-controlled room (22°C ± 1°C) with a 12-hour light/dark cycle and constant humidity. The mice had free access to tap water and rodent diets *ad libitum* during the duration of the experiment. Ethical guidelines set by the Ethical Committee of Charles University, Faculty of Pharmacy in Hradec Králové, were strictly followed to ensure the welfare of laboratory animals (Project number MSMT-5793/2021-2, approval date: 4 May 2021). All planned experiments were conducted in accordance with Czech Law No. 246/1992 Sb.

11.2. Biochemical analysis

Blood samples were collected from the *inferior vena cava*, followed by applying 100 µl of fresh blood into the Preventive Care Profile Plus cartridge test to measure liver enzymes, specifically ALT and AST with a VetScan2 device (Abaxis, Griesheim, Hesse, Germany).

11.3. Workflow of the western blot method

11.3.1. Tissue homogenization and protein isolation

The homogenization process and preparation of total (for measuring ICAM-1 protein) and membrane fractions (for evaluating ENG and VCAM-1 proteins) were performed. The protein concentration was determined using the bicinchoninic method. This method involves the formation of complexes between sodium salt of bicinchoninic acid (BCA) and copper ions, which are generated through the reaction of copper ions and peptide bond in an alkaline environment. Spectrophotometric determination was performed to measure protein concentration of the liver samples.

11.3.2. Western blot method

The first step was the preparation of the apparatus (Mini-PROTEAN® Tetra Cell kit;Bio-Rad Laboratories, Inc., CA, USA) which was made of two glasses and a stand (the thick glass was placed in the back and the thin glass in front). It was necessary to conduct a leaking test with Milli-Q water to check the tightness of the glasses on the stand prior to using the actual separating gel.

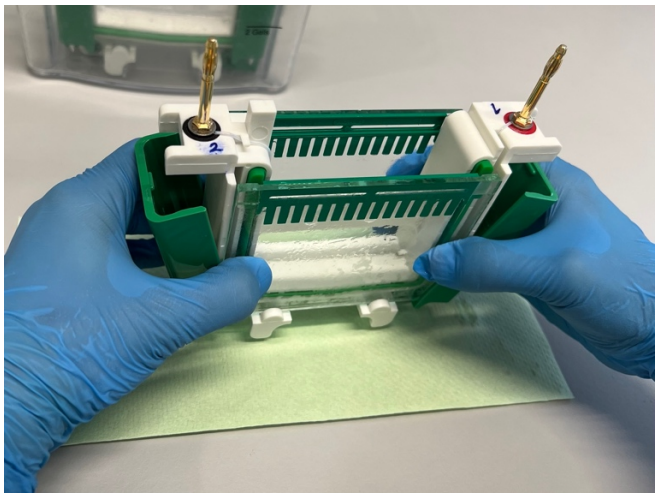

Figure 7: Proper assembly of the western blot apparatus

11.3.2.1. Gel preparation

Separating gel was prepared by mixing Milli-Q water, separating gel buffer, acrylamide-bis solution, 10% sodium-dodecyl sulphate (SDS), 10% ammonium persulphate (APS) and N,N,N',N'-tetramethylethylenediamine (TEMED). Once TEMED added the polymerization process started, so it is highly important to be pipetted in the last step. The concentration of the separating gel was determined according to the molecular weight of the targeted proteins and in this experiment the 10% concentration was used for ENG, ICAM-1, VCAM-1. Glyceraldehyde-3-phosphate dehydrogenase (GAPDH) used as the control protein in this experiment. The amount of each substance for preparation of two separating gels is shown in the Tab 1.

Table 1 composition of separation gels

components	**10% (ml)**
Milli-Q water	4.900
Separation gel buffer	2.500
Acrylamide-bis solution	2.500
10% SDS	0.100
10% APS	0.030
TEMED	0.015

The prepared separating gel was immediately (after the addition of TEMED) pipetted into the gap between the thick and thin glasses up to 1 cm below the upper edge of the thin glass. The remaining space was filled with isobutanol to avoid drying of the gel. The polymerization process of the gel lasted between 30 to 60 minutes. The isobutanol was washed away with Milli-Q water and the space above the gel was cautiously dried with filter paper.

The next step was the preparation of the stacking gel. The amount of the components for two gels (5%) is given in the Tab 2.

Table 2 composition of stacking gel

components	**5% (ml)**
Milli-Q water	6.150
Stacking gel buffer	2.500
Acrylamide-bis- solution	1.250
10% SDS	0.100
10% APS	0.030
TEMED	0.015

The prepared stacking gel was pipetted into the space between the separating gel and the upper edge of the thin glass, and all the bubbles were subsequently removed. Afterwards the Teflon comb was vertically inserted into the stacking gel following by filling the narrow space between the comb and the left and right corners of the glass by stacking gel. The second polymerization process took 30-60 minutes.

11.3.2.2. Sample preparation

14 samples and one marker (Precision Plus Protein ™Dual Colour Standards, Bio-Rad Laboratories, Inc., CA, USA) were diluted 1:1 with sample buffer (S3401, Sigma Aldrich, MO, USA) (6 µl sample + 6 µl sample buffer) for each gel. After preparation of the samples, they were kept on ice before the addition of buffer. The samples and marker were vortexed, centrifuged for 45 seconds at 5000 rpm following by boiling in a 95º water bath for 5 minutes. After reaching to the room temperature (10-15 min), samples and the marker centrifuged for another 30 seconds.

11.3.2.3. Gel electrophoresis

The set of glasses with polymerized gel was removed from the first apparatus and put into the stand for electrophoresis. Two gels would set on one stand by thin glasses facing each other. The stand was filled with running buffer and then placed on a dry napkin to ensure there were no leak. The running buffer was prepared by using 100 ml of 10x concentrated buffer (10x Tris/glycine/SDS, Bio-Rad Laboratories, Inc., CA, USA) added to 1000 ml of Milli-Q water. Once the stand was filled with buffer the Teflon combs were removed exactly vertical with cautious. The marker was applied to the first well of the gel from the left and all other wells were filled with samples (10 µl each) (figure 8). Two stands with two gels each, could be inserted into an electrophoresis tank by pointing so called "black to black, red to red". The tank was filled with running buffer and covered with a cap having electrodes again with the black and red color codes. The electrophoresis chamber system was connected to the power source according to the instructions provided in Tab 3. The last step was to shield all around the system with ice packs to protect the samples from heating up.

Table 3 parameters for setting electrophoretic conditions for 2 gels

Voltage	200 v
Electric current	120 mA
Time	35 minutes

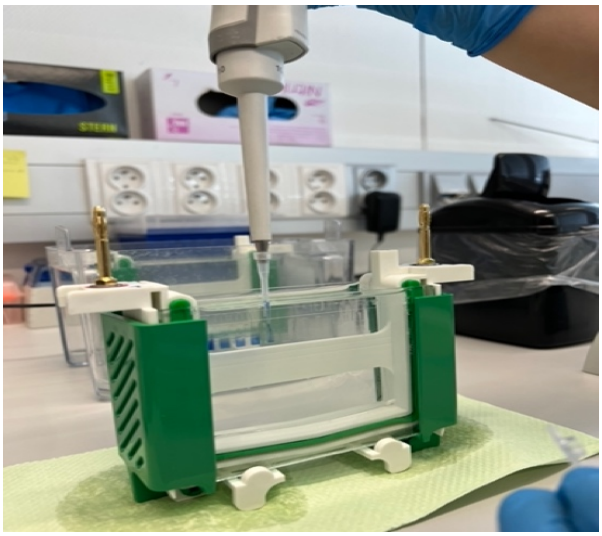

Figure 8: Application of marker and samples to wells with caution.

11.3.2.4. Wet blotting

Transfer buffer was prepared with 100 ml 10x concentrated buffer (10x Tris/Glycine/Buffer for western blots and Native Gels, Bio-Rad Laboratories, Inc., CA, USA), 200 ml methanol and 700 ml Milli-Q water. Due to exothermic reaction between transfer buffer and methanol, the transfer buffer was diluted with milli-Q water prior to addition of methanol.

The PVDF membrane (Immobilon®-E PVDF Membrane, Millipore, MA, USA) was used to transfer proteins. The membranes were cut to the determined cutting points on the membrane roll, and it was protected with a blue cover.

A tweezer was used to pull out the membranes gently from the cover and placed inside the Milli-Q water for 30 seconds on shaker for activation.

After the completion of the electrophoresis and disconnection from the power source, the stand with gels was removed from the system. The stand was opened, one gel pulled out to use and the other gel kept in the buffer. The glasses with the gel were separated from each other gently with the aid of a plastic spatula and after the separation, the glass with the gel was put inside a petri dish

with transfer buffer to remove the gel from the glass. The gel had to be in correct position in buffer (markers on the right). A cassette was used to build "sandwich" by the components in the following order: sponge, thick filter paper, gel, activated membrane, thick filter paper, sponge. (figure 9) A roller was used on the second thick filter paper to remove probable bubbles. All the components were soaked properly in the transfer buffer prior to sandwich formation. The cassette was sealed and implanted to a stand and the stand was placed inside the tank. The tank was poured with transfer buffer to the blotting point and covered with the lid according to the color code (like electrophoresis). The whole system was connected to the power source according to the condition given in Tab 4. Once again, the assembly was enclosed by ice packs.

Table 4 conditions for protein transfer

Voltage	140 V
Electric current	300 mA
Time	1,5 h

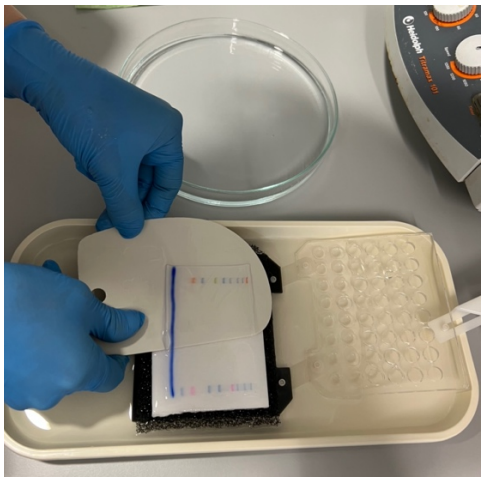

Figure 9: Placing the gel on activated membrane.

Once the process was finished, the system was disconnected from the power supply and the lid was removed. Subsequently, the cassette was pulled out and opened. The membrane sensibly separated from the gel and put inside the transfer buffer.

11.4. Immunodetection

11.4.1. Membrane blocking, primary and secondary antibodies

The TBS-T solution was prepared according to the following ratio: 100 ml of 10x concentrated Tris buffer saline (TBS), 900 ml Milli-Q water and 1 ml Tween20. It was important to pipette Tween20 with care due to its high viscosity. The TBS-T solution was thoroughly mixed on a magnetic stirrer.

Afterward, the blocking solution (5% milk) was prepared by mixing 5 g non-fat dry milk and 95 ml TBS-T. The mixture was then stirred on a magnetic stirrer.

The membrane was removed from the transfer buffer and placed on a ruler with the markers on its left side. It was then cut into few strips, with each strip referring to the molecular weight of targeted proteins.

The molecular wight of proteins used in this experiment is written in the tab 5.

Table 5 molecular weight of targeted proteins

ENG	95 kDa
ICAM-1	110 kDa
VCAM-1	110 kDa
GAPDH	36 kDa

The membrane strips were soaked in the 5% milk solution and incubated for 1 hour on shaker to block the whole membrane prior to the application of antibody.

Upon completion of the blocking process, the primary antibodies were able to specifically bound to the desired proteins. To achieve this, the required primary antibodies were diluted to the intended concentrations by 5% milk solution (Tab 6).

Table 6 concentration of primary antibodies

Primary antibody	***Host***	***Producer***	***Catalogue number***	***Dilution of the antibody***
ENG	*Rabbit*	*Abcam, Cambridge, UK*	*ab221675*	*1:1000*
ICAM-1	*Goat*	*R&D Systems, MN, USA*	*AF796*	*1:500*
VCAM-1	*Rabbit*	*Cell Signaling , MA, USA*	*32653s*	*1:1000*
GAPDH	*Rabbit*	*Cell Signaling, MA, USA*	*2118s*	*1:8000*

The diluted primary antibody applied on the strips and kept in fridge overnight. The next day, washing process took place by TBS-T solution 5 x 10 min. Afterwards, the secondary

antibodies were used with the given concentration (Tab 7) diluted by 5% milk. The secondary antibodies formed a complex with primary antibodies resulting in stained bands and aiding the identification of proteins.

Tab 7 concentration of secondary antibodies

Primary antibody	***Secondary antibody***	***producer***	***Catalogue number***	***Dilution of the antibody***
ENG	*Anti-rabbit*	*Abcam, Cam, UK*	*Ab6112*	*1:2000*
ICAM-1	*Anti-goat*	*Sigma Aldrich, MA, USA*	*A5420*	*1:4000*
VCAM-1	*Anti-rabbit*	*Abcam, Cam, UK*	*Ab6112*	*1:2000*
GAPDH	*Anti-rabbit*	*Cell Signaling, MA, USA*	*7074s*	*1:10000*

The membrane strips remained in the secondary antibodies on shaker for 1 hour and then washed again with TBS-T solution for 10 minutes 5 times.

11.5. Chemiluminescence detection

The final stage of western blot method was detection of the proteins. The chemiluminescent substrate utilized for the western blot analysis in this study was Immobilon Forte western HRP substrate (WBLUF0020, Merck, NJ, USA). This substrate is designed to react with horseradish peroxidase (HRP) enzyme-conjugated secondary antibodies, generating a luminescent signal that can be detected and quantified using an appropriate imaging system. The chemiluminescence solution was applied to the membrane strips. It was crucial to ensure complete coverage of the strip without any bubbles on the membrane surface. Details concerning the type of detection solution and its incubation time on the membrane strips are documented in Tab 8.

Table 8 chemiluminescence substrate

protein	Detection solution	Incubation (min)
ENG	Forte	2
ICAM-1	Forte	3
VCAM-1	Forte	3
GAPDH	Forte	3

Figure 10 Tools for chemiluminescence detection

Following the designated incubation time, the detection solution was removed from the membrane strip, enclosed with a plastic wrap, and any excess detection solution was removed by gently pressure and moving the hand on the plastic wrap. The assembly was subsequently put inside the ChemiDoc device.

As a result of the detection process, bands of different thickness and color intensity appeared, presenting shades ranging from grey to black.

Equal loading of proteins onto the gel was established by immunodetection of mouse monoclonal anti-GAPDH antibody. The bands were captured by ChemiDoc™ MP Imaging System (Bio-Rad Laboratories, Hercules, CA, USA). Image Lab software (Bio-Rad Laboratories, Hercules, CA, USA, version 6.0.1) was used to quantify the bands.

Figure 11: ChemiDoc™ MP Imaging System and Image Lab software

11.6. Statistical analysis

The statistical analysis for this research study was conducted using GraphPad Prism software version 9.2 (GraphPad Software Inc., San Diego, CA, USA). The data are presented as median values with the interquartile range. Group-to-group comparisons were performed using the non-parametric Mann-Whitney test, which is suitable for analyzing data that may not follow a normal distribution. Results with P-values less than 0.05 were statistically significant in this study. A bar graph was used to show the results, where the control group was represented by a green bar,

and the CD+IgG and CD+M1043 groups were represented by blue and red bars, respectively. The number that showed statistical significance was marked with a "*" (*$p \leq 0.05$, ** $p \leq 0.01$, *** $p \leq 0.001$).

12. Results

12.1.1. Effect of diet on liver enzyme, ALT levels, and the impact of M1043

The plasma level of ALT was measured to confirm liver injury in mice fed with a CDAA-HFD. A significant increase was found in the level of ALT in the plasma of mice fed with a CDAA-HFD when compared with the control group (Figure 12), suggesting liver impairment induced by the CDAA-HFD diet. In addition, there was no significant difference in ALT levels between CD+IgG and CD+M1043 groups. The results indicate that M1043 was not able to reduce ALT levels in CDAA-HFD-fed mice (Figure 12). These results suggest that CDAA-HFD induced liver injury in mice, which is confirmed by the significant increase in ALT levels. However, M1043 treatment did not have a significant effect on ALT levels in CDAA-HFD-fed mice.

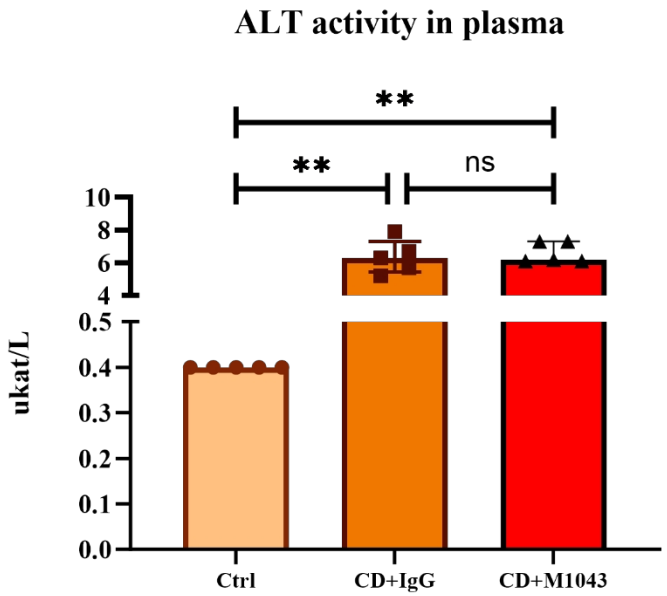

Figure 12. *ALT levels in the control group and two CDAA-HFD-fed groups. All data are shown as median with interquartile range. Mann-Whitney test, ** $p < 0.001$ ($n = 5$)*

12.1.2. Impact of CDAA-HFD on liver enzyme, AST levels, and the effect of M1043

The plasma level of AST was measured to confirm liver injury in mice fed with CDAA-HFD. The results showed a significant elevation of plasma levels of AST in CD+IgG and CD+M1043 mice compared to the chow diet group (Figure 13), suggesting liver impairment induced by the CDAA-HFD diet. However, there was no significant difference in AST levels between the CD+IgG and CD+M1043 groups (Figure 13). These findings indicate that CDAA-HFD leads to liver injury, as evidenced by the significant increase in AST levels. Furthermore, M1043 treatment did not have a significant impact on AST levels in CDAA-HFD-fed mice.

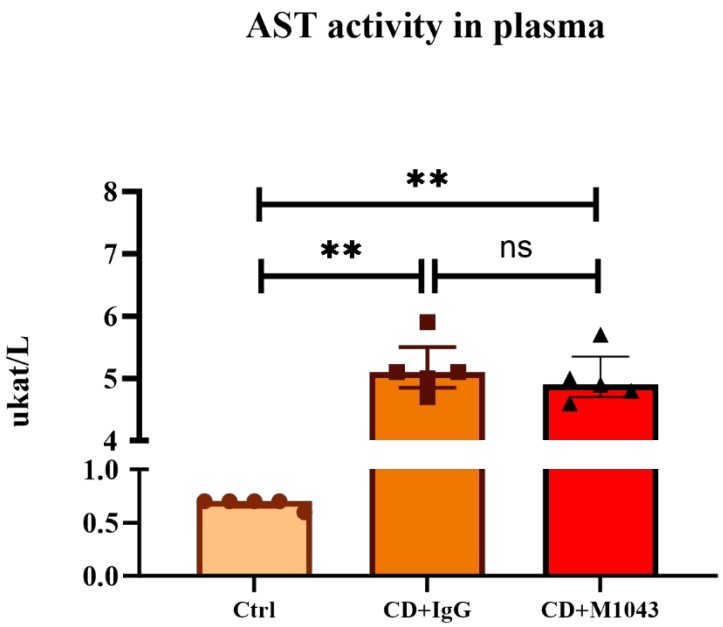

Figure 13. *AST levels in the control group and two CDAA-HFD-fed groups. All data are shown as median with interquartile range. Mann-Whitney test, ** $p < 0.001$ ($n = 5$)*

12.1.3. Effect of CDAA-HFD and M1043 treatment on the expression of liver sinusoidal endothelial dysfunction markers

Western blot analysis was used to examine the expression of LSED markers in the mice, including protein expression of ENG, VCAM-1, and ICAM-1.

12.1.4. CDAA-HFD and M1043 modulates ENG protein expression

The expression of ENG protein was analyzed using western blot analysis to investigate the effect of CDAA-HFD and M1043 on LSECs. The results showed a significant increase in the level of ENG protein expression in the CDAA-HFD-fed groups compared to the control group (Figure 14). However, M1043 treatment significantly prevented increase of ENG expression in CD+M1043 compared to CD+IgG mice (Figure 14). These findings suggest that the M1043 was able to prevent LSED damage in M1043-injected animals.

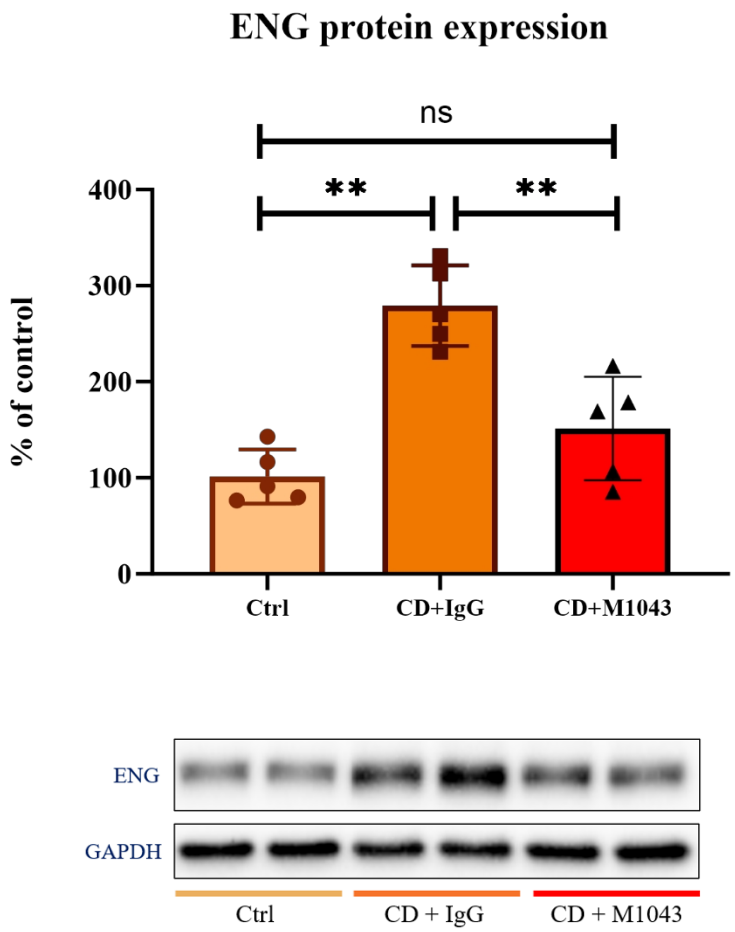

Figure 14. ENG *protein expression in mice liver. Densitometric quantification of immunoreactive bands (top panel: densitometric analysis, control = 100%) was recalculated to the* GAPDH *signal (bottom panel: representative immunoblots). All data are shown as median with interquartile range. Mann-Whitney test, ** $p < 0.01$ ($n = 5$).*

12.1.5. **Impact of CDAA-HFD and M1043 on protein expression of VCAM-1**

To explore the effect of CDAA-HFD and M1043 on liver damage, the expression of VCAM-1 protein was measured in liver samples using western blot analysis. The results showed a significant up-regulation of VCAM-1 in CDAA-HFD-fed mice compared to the control mice (Figure 15), suggesting liver damage induced by the CDAA-HFD diet. On the other hand, M1043

treatment significantly increase in VCAM-1 expression in CD+M1043 compared to CD+IgG mice (Figure 15), suggesting LSEC damage was prevented in M1043-injected mice.

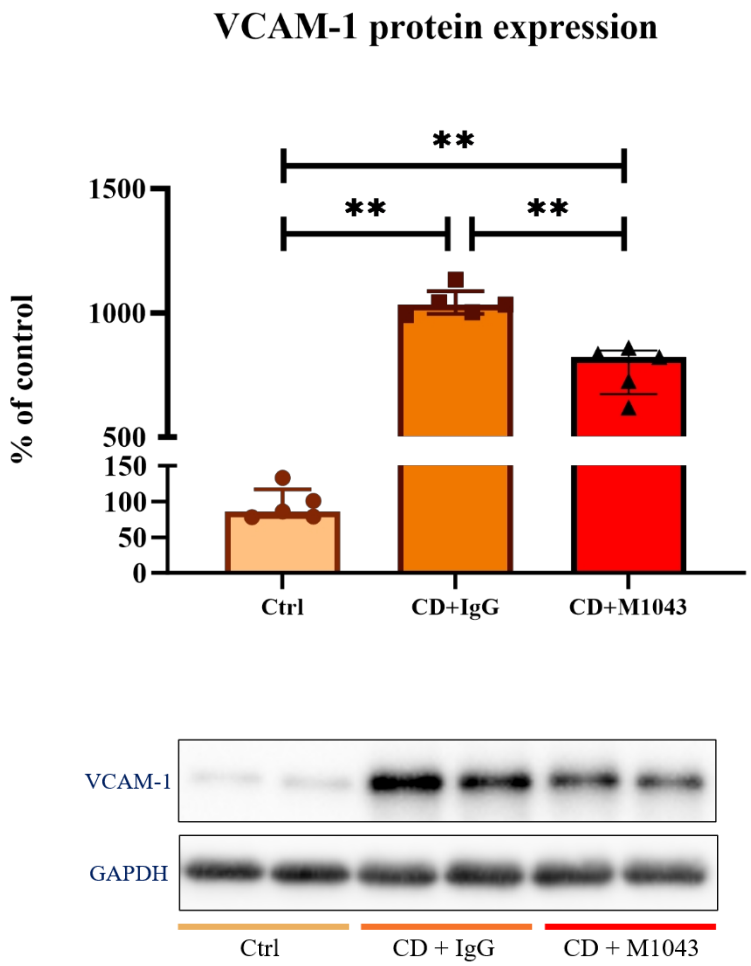

Figure 15. VCAM-1 *protein expression in mice liver. Densitometric quantification of immunoreactive bands (top panel: densitometric analysis, control = 100%) was recalculated to the* GAPDH *signal (bottom panel: representative immunoblots). All data are shown as median with interquartile range. Mann-Whitney test, ** $p < 0.01$ ($n = 5$).*

12.1.6. Effect of CDAA-HFD and M1043 treatment on protein Expression of ICAM-1

The effect of CDAA-HFD and M1043 on liver damage was investigated by measuring the expression of ICAM-1 proteins in liver samples using western blot analysis. The results showed a significant increase in the protein expression of ICAM-1 in the CDAA-HFD mice compared to the chow-fed group, suggesting LSEC impairment in CDAA-HFD-fed mice (Figure 16). Similarly, as in previous proteins, M1043 treatment significantly prevented increase in ICAM-1 expression in CD+M1043 compared to CD+IgG mice (Figure 16), proposing possible protection of M1043 against LSEC development.

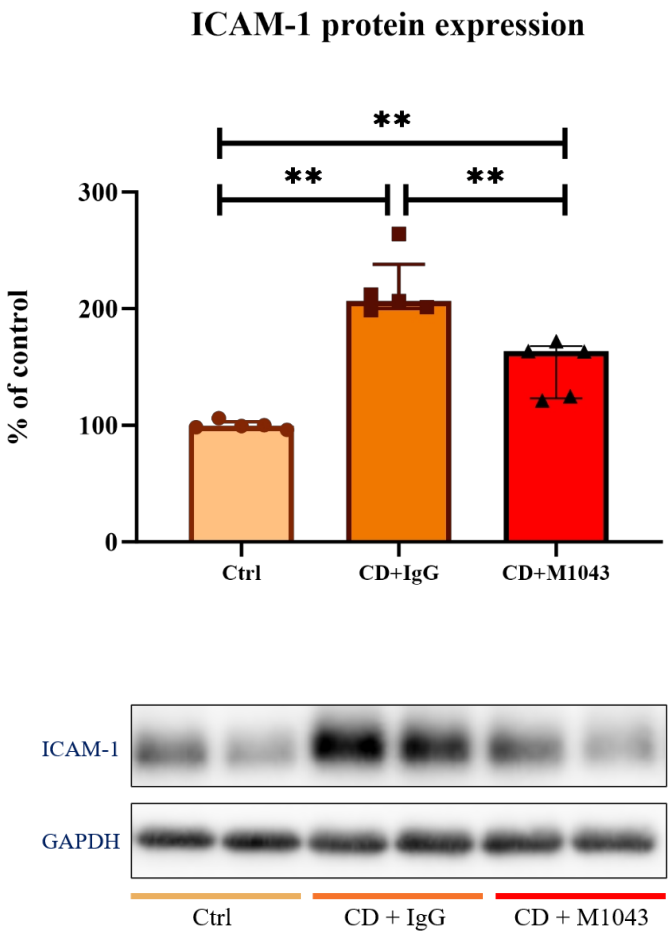

Figure 16. ICAM-1 *protein expression in mice liver. Densitometric quantification of immunoreactive bands (top panel: densitometric analysis, control = 100%) was recalculated to the* GAPDH *signal (bottom panel: representative immunoblots). All data are shown as median with interquartile range. Mann-Whitney test, ** $p < 0.01$ ($n = 5$).*

13. Discussion

The current study investigated the impact of CDAA-HFD on mice liver and evaluated the potential therapeutic effects of anti-ENG monoclonal antibody, M1043, as a novel therapeutic agent on NASH changes. The manifestation of ENG has been established in HSCs, Kupffer and endothelial cells previously [13]. Our findings have significant implication for understanding the pathogenesis of liver injury induced by CDAA-HFD and the potential role of M1043 on LSED in NASH changes. The study provides a comprehensive assessment of both functional and molecular aspect of liver injury, shedding light on the complex interplay between diet-induced liver damage and the therapeutic intervention with M1043.

Our results indicated that CDAA-HFD induced liver injury, as evidenced by significant increase in plasma levels of liver enzymes (ALT and AST), which are indicative of liver impairment. In addition, the study showed that M1043 treatment did not significantly affect ALT and AST levels in CDAA-HFD-fed mice, suggesting that it may not have a substantial impact on mitigating liver injury within this experimental framework, unless extended treatment durations are implanted.

Moreover, the study delves into the molecular mechanisms underlying LSED, a key aspect of hepatic injury. The western blot analysis revealed that CDAA-HFD leads to and upregulation of LSED markers, including ENG, VCAM-1, and ICAM-1. Importantly, M1043 treatment was found to significantly decrease the protein expression of these LSED markers in CDAA-HFD mice, indicating its potential to attenuate LSED damage and mitigate liver injury.

CDAA-HFD has been utilized to mimic human NASH in mice to recapitulate the accumulation of fat in the liver (steatosis), inflammation, and liver cell damage, which can lead to

fibrosis and eventually cirrhosis or liver cancer [60]. Interestingly, it has been demonstrated that CDAA-HFD shows a close resemblance of pathology to human's NASH [58].

M1043 (monoclonal rat anti-mouse ENG antibody) is a monoclonal antibody, specifically targeted against mouse ENG, a type III TGFβ co-receptor. The M1043 antibody was created to compete with mouse BMP binding and has been studied in mouse models to mimic the anticipated effect of such antibody in humans [69].

The CDAA-HFD diet in this study led to an increase in the expression of ENG in LSECs, consistent with the findings of Eissazadeh et al. (2023), who observed a similar increase in ENG expression in the same mouse model of diet-induced NASH [75]. Furthermore, several other studies have highlighted the involvement of ENG in the development of endothelial dysfunction and inflammation by facilitating leukocyte transmigration in various organs. For instance, Rossi et al. demonstrated that a decrease in ENG expression led to reduced inflammation-induced transendothelial migration of leukocytes, indicating the significant role of ENG in this process, which is a characteristic feature of endothelial dysfunction in organs such as the peritoneum or lungs [76]. It has been shown that blocking ENG with TRC105 inhibited invasion of cancer associated fibroblast (CAF) *in vitro*. Additionally, specific targeting of ENG in CAFs with TRC105 decreases the metastatic spread of colorectal cancer cells to the liver in mice [77]. Targeting malignant peripheral nerve sheath tumors with ENG-neutralizing antibodies (TRC105/M1043) resulted in a reduction of tumor growth and metastasis in xenograft models. This effect was achieved by attenuating tumor cell proliferation and angiogenesis [78]. Moreover, Tripska et al. demonstrated that blocking ENG with TRC105 can mitigate the endothelial dysfunction induced by hypercholesterolemia and hyperglycemia in human aortic endothelial cells [8]. All these studies suggest important role of ENG in endothelial dysfunction and sinusoidal

endothelial dysfunction. In our study, we observed a prevention of CDAA-HFD induced increase of ENG protein expression after four weeks of treatment with M1043, indicating successful effects of anti-ENG antibody which might indicate alleviation of LSED development after M1043 treatment.

In order to establish LSED development, we examined the expression of VCAM-1 and ICAM-1, recognized as biomarkers indicative of endothelial dysfunction progression [79]. We observed a significant upregulation of VCAM-1 in LSECs during the advancement of NASH [50] . Previous investigations have shown that the specific depletion of VCAM-1 in endothelial cells improved liver inflammation and reduced the infiltration of macrophages in carbon tetrachloride (CCl4)-induced liver NASH and fibrosis [80]. In alignment with these findings, our study revealed an increased expression of VCAM-1 in NASH mice, indicating its involvement in LSED. Indeed, we observed a reduced in VCAM-1 protein levels after four weeks of M1043 treatment suggesting that M1043 prevents CDAA-HFD induced increase of VCAM-1 in vivo. These results suggest that blocking ENG could effectively lower VCAM-1 levels, an inflammation marker linked to endothelial dysfunction, proposing M1043 antibody as a promising treatment for NASH changes.

ICAM-1 is a glycoprotein situated on the cellular membrane, function as an adhesive molecule pivotal in orchestrating inflammatory processes. It is involved in recruitment of immune cells to the inflamed locale functionally [6]. Furthermore, ICAM-1 assumes a significant role in governing inflammatory reaction and facilitating cellular interaction [81]. Based on our results, protein expression of ICAM-1 has been upregulated in NASH animals compared to control group, proposing its participation in NASH enhancement. Similarly, as for ENG and VCAM-1, M1043 treatment prevented the protein expression of ICAM-1 increase in CDAA-HFD mice, suggesting

the potential of this monoclonal antibody as an effective approach for mitigating NASH development.

However, further research is warranted to elucidate the precise mechanisms underlying the observed effect and to evaluate the translational potential of M1043 as a therapeutic agent for liver injury.

14. Conclusion

The study delved into the impact of CDAA-HFD on mouse liver and explored the therapeutic potential of the ENG monoclonal antibody, M1043, as a novel treatment for NASH. The finding significantly enhances our understanding of liver injury by CDAA-HFD and shed light on M1043's potential in mitigating LSED. The research comprehensively evaluated both functional and molecular aspects of liver injury, emphasizing the intricate relationship between diet-induced liver damage and therapeutic intervention with M1043.

The results revealed that CDAA-HFD led to liver injury, evidenced by a notable increase in plasma levels of liver enzymes (ALT and AST), indicating liver impairment. M1043 treatment did not markedly impact ALT and AST levels in NASH mice in this study. Additionally, the study explored the molecular mechanisms underlying LSED, showing an upregulation of LSED markers, including ENG, VCAM-1, and ICAM-1 in CDAA-HFD fed mice. Interestingly, M1043 treatment significantly prevented CDAA-HFD induced increase in the protein expression of these LSED markers, suggesting its potential to alleviate LSED damage and mitigate liver injury.

We can conclude that our research outcomes align with prior studies indicating ENG's involvement in endothelial dysfunction and inflammation across various pathologies. Moreover, our findings propose that blocking ENG with M1043 could effectively decrease protein expression of ENG, marker of endothelial dysfunction, VCAM-1 and ICAM, biomarkers of inflammation associated with endothelial dysfunction, offering M1043 as a potential therapeutic intervention for NASH development.

List of tables:

List of figures:

15. References

[1] T. Huby and E. L. Gautier, "Immune cell-mediated features of non-alcoholic steatohepatitis," *Nat Rev Immunol*, vol. 22, no. 7, pp. 429–443, Jul. 2022, doi: 10.1038/s41577-021-00639-3.

[2] K.-S. Jeng, I.-S. Sheen, S.-S. Lin, C.-M. Leu, and C.-F. Chang, "The Role of Endoglin in Hepatocellular Carcinoma," *Int J Mol Sci*, vol. 22, no. 6, p. 3208, Mar. 2021, doi: 10.3390/ijms22063208.

[3] I. C. Igreja Sá *et al.*, "Soluble Endoglin as a Potential Biomarker of Nonalcoholic Steatohepatitis (NASH) Development, Participating in Aggravation of NASH-Related Changes in Mouse Liver," *Int J Mol Sci*, vol. 21, no. 23, p. 9021, Nov. 2020, doi: 10.3390/ijms21239021.

[4] M. Vicen *et al.*, "Membrane and soluble endoglin role in cardiovascular and metabolic disorders related to metabolic syndrome," *Cell. Mol. Life Sci.*, vol. 78, no. 6, pp. 2405–2418, Mar. 2021, doi: 10.1007/s00018-020-03701-w.

[5] E. Dolezelova *et al.*, "High soluble endoglin levels regulate cholesterol homeostasis and bile acids turnover in the liver of transgenic mice," *Life Sciences*, vol. 232, p. 116643, Sep. 2019, doi: 10.1016/j.lfs.2019.116643.

[6] T. M. Bui, H. L. Wiesolek, and R. Sumagin, "ICAM-1: A master regulator of cellular responses in inflammation, injury resolution, and tumorigenesis," *J Leukoc Biol*, vol. 108, no. 3, pp. 787–799, Sep. 2020, doi: 10.1002/JLB.2MR0220-549R.

[7] K. Furuta *et al.*, "Lipid-induced endothelial vascular cell adhesion molecule 1 promotes nonalcoholic steatohepatitis pathogenesis," *J Clin Invest*, vol. 131, no. 6, p. e143690, doi: 10.1172/JCI143690.

[8] K. Tripska *et al.*, "Monoclonal anti-endoglin antibody TRC105 (carotuximab) prevents hypercholesterolemia and hyperglycemia-induced endothelial dysfunction in human aortic endothelial cells," *Front Med (Lausanne)*, vol. 9, p. 845918, Sep. 2022, doi: 10.3389/fmed.2022.845918.

[9] M. J. A. Schoonderwoerd, M.-J. T. H. Goumans, and L. J. A. C. Hawinkels, "Endoglin: Beyond the Endothelium," *Biomolecules*, vol. 10, no. 2, p. 289, Feb. 2020, doi: 10.3390/biom10020289.

[10] R. S, M. A, B. Nn, and D. R, "A comprehensive study and extensive review of morphological variations of liver with new insights," *Surgical and radiologic anatomy : SRA*, vol. 44, no. 3, Mar. 2022, doi: 10.1007/s00276-022-02883-1.

[11] M. Mosharaf-Dehkordi, "A fully coupled porous media and channels flow approach for simulation of blood and bile flow through the liver lobules," *Computer Methods in Biomechanics and Biomedical Engineering*, vol. 22, no. 9, pp. 901–915, Jul. 2019, doi: 10.1080/10255842.2019.1601180.

[12] "Liver | Functions, Diseases & Treatments | Britannica." Accessed: Jan. 13, 2024. [Online]. Available: https://www.britannica.com/science/liver

[13] C. Lau *et al.*, "The Voronoi theory of the normal liver lobular architecture and its applicability in hepatic zonation," *Sci Rep*, vol. 11, p. 9343, Apr. 2021, doi: 10.1038/s41598-021-88699-2.

[14] E. Trefts, M. Gannon, and D. H. Wasserman, "The liver," *Curr Biol*, vol. 27, no. 21, pp. R1147–R1151, Nov. 2017, doi: 10.1016/j.cub.2017.09.019.

[15] L. E. Greenbaum, C. Ukomadu, and J. S. Tchorz, “Clinical translation of liver regeneration therapies: A conceptual road map,” *Biochemical Pharmacology*, vol. 175, p. 113847, May 2020, doi: 10.1016/j.bcp.2020.113847.

[16] S. O. Jensen-Cody and M. J. Potthoff, “Hepatokines and metabolism: Deciphering communication from the liver,” *Mol Metab*, vol. 44, p. 101138, Dec. 2020, doi: 10.1016/j.molmet.2020.101138.

[17] E. Van Peer *et al.*, “In vitro Phase I- and Phase II-Drug Metabolism in The Liver of Juvenile and Adult Göttingen Minipigs,” *Pharm Res*, vol. 34, no. 4, pp. 750–764, Apr. 2017, doi: 10.1007/s11095-017-2101-y.

[18] B. G. Lake and R. J. Price, “Evaluation of the metabolism and hepatotoxicity of xenobiotics utilizing precision-cut slices,” *Xenobiotica*, vol. 43, no. 1, pp. 41–53, Jan. 2013, doi: 10.3109/00498254.2012.734643.

[19] S. J. Burwen, D. L. Schmucker, and A. L. Jones, “Subcellular and molecular mechanisms of bile secretion,” *Int Rev Cytol*, vol. 135, pp. 269–313, 1992, doi: 10.1016/s0074-7696(08)62043-4.

[20] J. J. G. Marin, R. I. R. Macias, O. Briz, J. M. Banales, and M. J. Monte, “Bile Acids in Physiology, Pathology and Pharmacology,” *Curr Drug Metab*, vol. 17, no. 1, pp. 4–29, 2015, doi: 10.2174/1389200216666151103115454.

[21] J. L. Boyer, “Bile Formation and Secretion,” *Compr Physiol*, vol. 3, no. 3, pp. 1035–1078, Jul. 2013, doi: 10.1002/cphy.c120027.

[22] “The immune niche of the liver | Clinical Science | Portland Press.” Accessed: Nov. 25, 2023. [Online]. Available: https://portlandpress.com/clinsci/article/135/20/2445/230035/The-immune-niche-of-the-liver

[23] P. Kubes and C. Jenne, “Immune Responses in the Liver,” *Annu. Rev. Immunol.*, vol. 36, no. 1, pp. 247–277, Apr. 2018, doi: 10.1146/annurev-immunol-051116-052415.

[24] L. Kořínková *et al.*, “Pathophysiology of NAFLD and NASH in Experimental Models: The Role of Food Intake Regulating Peptides,” *Front Endocrinol (Lausanne)*, vol. 11, p. 597583, Nov. 2020, doi: 10.3389/fendo.2020.597583.

[25] M. V. Chakravarthy and B. A. Neuschwander□Tetri, “The metabolic basis of nonalcoholic steatohepatitis,” *Endocrinol Diabetes Metab*, vol. 3, no. 4, p. e00112, Feb. 2020, doi: 10.1002/edm2.112.

[26] G. T. Brown and D. E. Kleiner, “Histopathology of Nonalcoholic Fatty Liver Disease and Nonalcoholic Steatohepatitis,” *Metabolism*, vol. 65, no. 8, pp. 1080–1086, Aug. 2016, doi: 10.1016/j.metabol.2015.11.008.

[27] D. E. Kleiner and H. R. Makhlouf, “Histology of NAFLD and NASH in Adults and Children,” *Clin Liver Dis*, vol. 20, no. 2, pp. 293–312, May 2016, doi: 10.1016/j.cld.2015.10.011.

[28] E. Hashimoto, M. Taniai, and K. Tokushige, “Characteristics and diagnosis of NAFLD/NASH,” *J Gastroenterol Hepatol*, vol. 28 Suppl 4, pp. 64–70, Dec. 2013, doi: 10.1111/jgh.12271.

[29] V. A. Piazzolla and A. Mangia, “Noninvasive Diagnosis of NAFLD and NASH,” *Cells*, vol. 9, no. 4, p. 1005, Apr. 2020, doi: 10.3390/cells9041005.

[30] E. E. Powell, V. W.-S. Wong, and M. Rinella, “Non-alcoholic fatty liver disease,” *The Lancet*, vol. 397, no. 10290, pp. 2212–2224, Jun. 2021, doi: 10.1016/S0140-6736(20)32511-3.

[31] L. J. M. Heyens, D. Busschots, G. H. Koek, G. Robaeys, and S. Francque, “Liver Fibrosis in Non-alcoholic Fatty Liver Disease: From Liver Biopsy to Non-invasive Biomarkers in

Diagnosis and Treatment," *Front Med (Lausanne)*, vol. 8, p. 615978, Apr. 2021, doi: 10.3389/fmed.2021.615978.

[32] X. Guo, X. Yin, Z. Liu, and J. Wang, "Non-Alcoholic Fatty Liver Disease (NAFLD) Pathogenesis and Natural Products for Prevention and Treatment," *International Journal of Molecular Sciences*, vol. 23, no. 24, Art. no. 24, Jan. 2022, doi: 10.3390/ijms232415489.

[33] A. Alt *et al.*, "Structural and Functional Insights into Endoglin Ligand Recognition and Binding," *PLoS One*, vol. 7, no. 2, p. e29948, Feb. 2012, doi: 10.1371/journal.pone.0029948.

[34] R. I. Koleva *et al.*, "Endoglin Structure and Function," *Journal of Biological Chemistry*, vol. 281, no. 35, pp. 25110–25123, Sep. 2006, doi: 10.1074/jbc.M601288200.

[35] M. J. A. Schoonderwoerd *et al.*, "Targeting Endoglin-Expressing Regulatory T Cells in the Tumor Microenvironment Enhances the Effect of PD1 Checkpoint Inhibitor Immunotherapy," *Clin Cancer Res*, vol. 26, no. 14, pp. 3831–3842, Jul. 2020, doi: 10.1158/1078-0432.CCR-19-2889.

[36] S. Velasco *et al.*, "L- and S-endoglin differentially modulate TGFbeta1 signaling mediated by ALK1 and ALK5 in L6E9 myoblasts," *J Cell Sci*, vol. 121, no. Pt 6, pp. 913–919, Mar. 2008, doi: 10.1242/jcs.023283.

[37] E. Gallardo-Vara *et al.*, "Endoglin Protein Interactome Profiling Identifies TRIM21 and Galectin-3 as New Binding Partners," *Cells*, vol. 8, no. 9, p. 1082, Sep. 2019, doi: 10.3390/cells8091082.

[38] E. Fonsatti and M. Maio, "Highlights on endoglin (CD105): from basic findings towards clinical applications in human cancer," *Journal of Translational Medicine*, vol. 2, no. 1, p. 18, Jun. 2004, doi: 10.1186/1479-5876-2-18.

[39] S. K. Kim, M. A. Henen, and A. P. Hinck, "Structural biology of betaglycan and endoglin, membrane-bound co-receptors of the TGF-beta family," *Exp Biol Med (Maywood)*, vol. 244, no. 17, pp. 1547–1558, Dec. 2019, doi: 10.1177/1535370219881160.

[40] K. W. Finnson and A. Philip, "Endoglin in liver fibrosis," *J Cell Commun Signal*, vol. 6, no. 1, pp. 1–4, Mar. 2012, doi: 10.1007/s12079-011-0154-y.

[41] M. Alsamman *et al.*, "Endoglin in human liver disease and murine models of liver fibrosis —A protective factor against liver fibrosis," *Liver Int*, vol. 38, no. 5, pp. 858–867, May 2018, doi: 10.1111/liv.13595.

[42] A. Kasprzak and A. Adamek, "Role of Endoglin (CD105) in the Progression of Hepatocellular Carcinoma and Anti-Angiogenic Therapy," *Int J Mol Sci*, vol. 19, no. 12, p. 3887, Dec. 2018, doi: 10.3390/ijms19123887.

[43] F. About *et al.*, "Identification of an Endoglin Variant Associated With HCV-Related Liver Fibrosis Progression by Next-Generation Sequencing," *Front Genet*, vol. 10, p. 1024, Nov. 2019, doi: 10.3389/fgene.2019.01024.

[44] L. Kang, M. Kim, and Y. M. Lee, "Expression of ICAM-1 in Blood Vascular Endothelium and Tissues in Human Premalignant Lesion and Gastric/Hepatocellular Carcinomas," *Korean J Gastroenterol*, vol. 79, no. 4, pp. 170–176, Apr. 2022, doi: 10.4166/kjg.2022.008.

[45] S. Ito, T. Yukawa, S. Uetake, and M. Yamauchi, "Serum intercellular adhesion molecule-1 in patients with nonalcoholic steatohepatitis: comparison with alcoholic hepatitis," *Alcohol Clin Exp Res*, vol. 31, no. 1 Suppl, pp. S83-87, Jan. 2007, doi: 10.1111/j.1530-0277.2006.00292.x.

[46] A. Benedicto *et al.*, "Liver sinusoidal endothelial cell ICAM-1 mediated tumor/endothelial crosstalk drives the development of liver metastasis by initiating inflammatory and angiogenic responses," *Sci Rep*, vol. 9, p. 13111, Sep. 2019, doi: 10.1038/s41598-019-49473-7.

[47] Y. Duan *et al.*, "Association of Inflammatory Cytokines With Non-Alcoholic Fatty Liver Disease," *Front Immunol*, vol. 13, p. 880298, May 2022, doi: 10.3389/fimmu.2022.880298.

[48] N. Selzner, M. Selzner, B. Odermatt, Y. Tian, N. Van Rooijen, and P.-A. Clavien, "ICAM-1 triggers liver regeneration through leukocyte recruitment and Kupffer cell-dependent release of TNF-alpha/IL-6 in mice," *Gastroenterology*, vol. 124, no. 3, pp. 692–700, Mar. 2003, doi: 10.1053/gast.2003.50098.

[49] A. Lembas, K. Zawartko, M. Sapuła, T. Mikuła, J. Kozłowska, and A. Wiercińska-Drapało, "VCAM-1 as a Biomarker of Endothelial Function among HIV-Infected Patients Receiving and Not Receiving Antiretroviral Therapy," *Viruses*, vol. 14, no. 3, p. 578, Mar. 2022, doi: 10.3390/v14030578.

[50] R. M. Carr, "VCAM-1: closing the gap between lipotoxicity and endothelial dysfunction in nonalcoholic steatohepatitis," *The Journal of Clinical Investigation*, vol. 131, no. 6, Mar. 2021, doi: 10.1172/JCI147556.

[51] S. Lefere *et al.*, "Serum vascular cell adhesion molecule-1 predicts significant liver fibrosis in non-alcoholic fatty liver disease," *Int J Obes*, vol. 41, no. 8, Art. no. 8, Aug. 2017, doi: 10.1038/ijo.2017.102.

[52] M. Nachit *et al.*, "Molecular imaging of liver inflammation using an anti-VCAM-1 nanobody," *Nat Commun*, vol. 14, no. 1, Art. no. 1, Feb. 2023, doi: 10.1038/s41467-023-36776-7.

[53] “Elevated Expression of Serum Endothelial Cell Adhesion Molecules in COVID-19 Patients - PMC.” Accessed: Dec. 20, 2023. [Online]. Available: https://www.ncbi.nlm.nih.gov/pmc/articles/PMC7337874/

[54] J. Poisson *et al.*, “Liver sinusoidal endothelial cells: Physiology and role in liver diseases,” *Journal of Hepatology*, vol. 66, no. 1, pp. 212–227, Jan. 2017, doi: 10.1016/j.jhep.2016.07.009.

[55] J. Gracia-Sancho, E. Caparrós, A. Fernández-Iglesias, and R. Francés, “Role of liver sinusoidal endothelial cells in liver diseases,” *Nat Rev Gastroenterol Hepatol*, vol. 18, no. 6, pp. 411–431, Jun. 2021, doi: 10.1038/s41575-020-00411-3.

[56] N. Nasiri-Ansari *et al.*, “Endothelial Cell Dysfunction and Nonalcoholic Fatty Liver Disease (NAFLD): A Concise Review,” *Cells*, vol. 11, no. 16, p. 2511, Aug. 2022, doi: 10.3390/cells11162511.

[57] M. A. Van Herck, L. Vonghia, and S. M. Francque, “Animal Models of Nonalcoholic Fatty Liver Disease—A Starter’s Guide,” *Nutrients*, vol. 9, no. 10, p. 1072, Sep. 2017, doi: 10.3390/nu9101072.

[58] C.-M. Flessa *et al.*, “Genetic and Diet-Induced Animal Models for Non-Alcoholic Fatty Liver Disease (NAFLD) Research,” *Int J Mol Sci*, vol. 23, no. 24, p. 15791, Dec. 2022, doi: 10.3390/ijms232415791.

[59] S. H. Ibrahim, P. Hirsova, H. Malhi, and G. J. Gores, “Animal Models of Nonalcoholic Steatohepatitis: Eat, Delete, and Inflame,” *Dig Dis Sci*, vol. 61, no. 5, pp. 1325–1336, May 2016, doi: 10.1007/s10620-015-3977-1.

[60] M. Matsumoto *et al.*, "An improved mouse model that rapidly develops fibrosis in non-alcoholic steatohepatitis," *Int J Exp Pathol*, vol. 94, no. 2, pp. 93–103, Apr. 2013, doi: 10.1111/iep.12008.

[61] M. Tsujie *et al.*, "Anti-tumor activity of an anti-endoglin monoclonal antibody is enhanced in immunocompetent mice," *Int J Cancer*, vol. 122, no. 10, pp. 2266–2273, May 2008, doi: 10.1002/ijc.23314.

[62] H. H. Hansen, M. Feigh, S. S. Veidal, K. T. Rigbolt, N. Vrang, and K. Fosgerau, "Mouse models of nonalcoholic steatohepatitis in preclinical drug development," *Drug Discovery Today*, vol. 22, no. 11, pp. 1707–1718, Nov. 2017, doi: 10.1016/j.drudis.2017.06.007.

[63] S. Uneda *et al.*, "Anti-endoglin monoclonal antibodies are effective for suppressing metastasis and the primary tumors by targeting tumor vasculature," *International journal of cancer. Journal international du cancer*, vol. 125, no. 6, p. 1446, Sep. 2009, doi: 10.1002/ijc.24482.

[64] H. Kaplon and J. M. Reichert, "Antibodies to watch in 2018," *MAbs*, vol. 10, no. 2, pp. 183–203, Jan. 2018, doi: 10.1080/19420862.2018.1415671.

[65] Y. Liu, M. Paauwe, A. B. Nixon, and L. J. A. C. Hawinkels, "Endoglin Targeting: Lessons Learned and Questions That Remain," *Int J Mol Sci*, vol. 22, no. 1, p. 147, Dec. 2020, doi: 10.3390/ijms22010147.

[66] R. L. Jones *et al.*, "Efficacy and Safety of TRC105 Plus Pazopanib vs Pazopanib Alone for Treatment of Patients With Advanced Angiosarcoma: A Randomized Clinical Trial," *JAMA Oncol*, vol. 8, no. 5, pp. 740–747, May 2022, doi: 10.1001/jamaoncol.2021.3547.

[67] D. Ag *et al.*, "Phase I and Preliminary Phase II Study of TRC105 in Combination with Sorafenib in Hepatocellular Carcinoma," *Clinical cancer research : an official journal of the*

American Association for Cancer Research, vol. 23, no. 16, Aug. 2017, doi: 10.1158/1078-0432.CCR-16-3171.

[68] H.-W. Wu *et al.*, "Anti-CD105 Antibody Eliminates Tumor Microenvironment Cells and Enhances Anti-GD2 Antibody Immunotherapy of Neuroblastoma with Activated Natural Killer Cells," *Clin Cancer Res*, vol. 25, no. 15, pp. 4761–4774, Aug. 2019, doi: 10.1158/1078-0432.CCR-18-3358.

[69] O. Nolan-Stevaux *et al.*, "Endoglin Requirement for BMP9 Signaling in Endothelial Cells Reveals New Mechanism of Action for Selective Anti-Endoglin Antibodies," *PLoS ONE*, vol. 7, no. 12, 2012, doi: 10.1371/journal.pone.0050920.

[70] S. Kumar *et al.*, "Antibody-directed coupling of endoglin and MMP-14 is a key mechanism for endoglin shedding and deregulation of TGF-β signaling," *Oncogene*, vol. 33, no. 30, pp. 3970–3979, Jul. 2014, doi: 10.1038/onc.2013.386.

[71] T. S. Hnasko and R. M. Hnasko, "The Western Blot," *Methods Mol Biol*, vol. 1318, pp. 87–96, 2015, doi: 10.1007/978-1-4939-2742-5_9.

[72] G. H. Meftahi, Z. Bahari, A. Zarei Mahmoudabadi, M. Iman, and Z. Jangravi, "Applications of western blot technique: From bench to bedside," *Biochemistry and Molecular Biology Education*, vol. 49, no. 4, pp. 509–517, 2021, doi: 10.1002/bmb.21516.

[73] T. Mahmood and P.-C. Yang, "Western Blot: Technique, Theory, and Trouble Shooting," *North American Journal of Medical Sciences*, vol. 4, no. 9, p. 429, Sep. 2012, doi: 10.4103/1947-2714.100998.

[74] P. Modi, A. Thepa, N. Jamir, and S. Yenisetti, "Extraction and processing of fly brain proteins for western blotting," 2022, pp. 381–388.

[75] S. Eissazadeh *et al.*, "Endoglin and soluble endoglin in liver sinusoidal endothelial dysfunction in vivo," *Biochimica et Biophysica Acta (BBA) - Molecular Basis of Disease*, vol. 1870, no. 3, p. 166990, Mar. 2024, doi: 10.1016/j.bbadis.2023.166990.

[76] "Endothelial endoglin is involved in inflammation: role in leukocyte adhesion and transmigration | Blood | American Society of Hematology." Accessed: Mar. 03, 2024. [Online]. Available: https://ashpublications.org/blood/article/121/2/403/30977/Endothelial-endoglin-is-involved-in-inflammation

[77] M. Paauwe *et al.*, "Endoglin Expression on Cancer-Associated Fibroblasts Regulates Invasion and Stimulates Colorectal Cancer Metastasis," *Clinical Cancer Research*, vol. 24, no. 24, pp. 6331–6344, Dec. 2018, doi: 10.1158/1078-0432.CCR-18-0329.

[78] "Endoglin, a Novel Biomarker and Therapeutical Target to Prevent Malignant Peripheral Nerve Sheath Tumor Growth and Metastasis | Clinical Cancer Research | American Association for Cancer Research." Accessed: Mar. 03, 2024. [Online]. Available: https://aacrjournals.org/clincancerres/article-abstract/29/18/3744/728900/Endoglin-a-Novel-Biomarker-and-Therapeutical

[79] E. Hintermann and U. Christen, "The Many Roles of Cell Adhesion Molecules in Hepatic Fibrosis," *Cells*, vol. 8, no. 12, Art. no. 12, Dec. 2019, doi: 10.3390/cells8121503.

[80] Q. Guo *et al.*, "Liver sinusoidal endothelial cell expressed vascular cell adhesion molecule 1 promotes liver fibrosis," *Frontiers in Immunology*, vol. 13, 2022, Accessed: Mar. 03, 2024. [Online]. Available: https://www.frontiersin.org/journals/immunology/articles/10.3389/fimmu.2022.983255

[81] H. Harjunpää, M. Llort Asens, C. Guenther, and S. C. Fagerholm, "Cell Adhesion Molecules and Their Roles and Regulation in the Immune and Tumor Microenvironment,"

Frontiers in Immunology, vol. 10, 2019, Accessed: Mar. 03, 2024. [Online]. Available: https://www.frontiersin.org/journals/immunology/articles/10.3389/fimmu.2019.01078